Geology of the Moscow Landing Section, Tombigbee River, Western Alabama, with Focus on Ichnologic Aspects of the Lower Paleocene Clayton Formation

by

Carleton Barrett Foster III

A thesis submitted to the Graduate Faculty of
Auburn University
in partial fulfillment of the
requirements for the Degree of
Master of Science

Auburn, Alabama
August 3, 2019

Keywords: sedimentology, ichnology,
map, carbonates, Paleogene

Approved by

Dr. Charles E. Savrda, Chair, Professor of Geology
Dr. Ronald D. Lewis, Associate Professor of Geology
Dr. David T. King Jr., Professor of Geology

Abstract

Sedimentologic and ichnologic studies were performed on units of the Moscow Landing section, a ~1.5-km exposure of Upper Cretaceous and Lower Paleocene strata along the west bank of the Tombigbee River, Sumter County, Alabama. Goals of the study were (1) to generate a detailed geologic map of the entire Moscow Landing exposure, (2) to characterize and interpret large burrow systems expressed in an alternating marl/marly limestone sequence in the middle portion of the Clayton Formation, and (3) to characterize the sedimentology and ichnology of a thin chalk bed (referred to as the “Clayton chalk”) in the upper part of the Clayton Formation.

This study produced the first detailed map of the Moscow Landing section, which should benefit future visitors to the site. The map, comprising nine partly overlapping segments or strips, depicts the distribution of stratigraphic units (upper part of the Prairie Bluff Chalk, discontinuous Clayton sand bodies, the Clayton Formation, lower part of the Porters Creek Formation, and select marker beds therein) and structural features (faults and bedding attitudes).

Large, highly irregular, branching burrow systems hosted in Clayton Formation marls are attributed to decapod crustaceans and assigned to the ichnotaxa *Spongeliomorpha iberica* and *Thalassinoides paradoxicus*. Both of these forms are indicative of the firmground Glossifungites ichnofacies.

Consistent with previous sequence stratigraphic interpretations, firmground conditions developed in response to erosional exhumation of semiconsolidated marls at parasequence-bounding marine flooding surfaces, which are marked by limestone interbeds.

The Clayton chalk is characterized by a Zoophycos ichnofacies assemblage of traces. Compared to chalk-dominated units of the Cretaceous Selma Group in the eastern Gulf coastal plain, the Clayton chalk is most similar to the Demopolis Chalk with respect to sediment texture, composition, and ichnofabric. This suggests that the Clayton chalk was deposited in a relatively quiet, outer-shelf setting. Based on biostratigraphic constraints, the transgression responsible for Clayton chalk deposition occurred ~62-63 Myr ago and is in part coeval with the development of the Cannonball Sea in the U.S. Western Interior. The transition from Clayton chalk to clay-dominated Porters Creek deposits reflects relatively abrupt changes in sea-level, paleogeography, and depositional environments along the eastern flank of the Mississippi embayment.

Acknowledgments

First, I would like to thank the faculty members of the Auburn University Department of Geosciences for giving me this opportunity to advance my academic career. It has been a privilege to grow alongside the Department. I owe a special thank you to my advisor, Dr. Savrda, who has been a truly amazing mentor. His work ethic, diligence, dedication, and overall character are an inspiration to me. I wish that I had his talent as a wordsmith so that I could convey just how crucial his guidance and support have been. Thank you for believing in me. To Dr. Lewis and Dr. King, thank you for serving on my committee and for providing counsel throughout my work on this project and my academic career at Auburn University. Thank you to undergraduate assistants Edward DeMetz, Wesley Sandlin, and Colt Morton who provided invaluable aid in the field and in the lab. Thanks also to John Whitmore for providing field assistance and sharing his knowledge of structural geology. Without their help, I would still be excavating burrow systems and lugging block samples. To the staff of the Department of Geosciences, thank you for helping me with day-to-day tasks and, more importantly, for the untiring assistance and support you provide to the Department. To my fellow graduate students, I could not have hoped for a better group of people to spend the last two years with. I am grateful for the memories we made together. I am grateful also for our experiences that we don't

remember. Thank you to my family who have given me love and support since the beginning. To Anabelle Kline, you were there for me when I needed it the most. I can’t thank you enough. Lastly, I would like to thank the American Chemical Society-Petroleum Research Fund, Alabama Geological Society, and Department of Geosciences Advisory Board for providing financial support for my research.

Table of Contents

List of Tables

List of Figures

List of Abbreviations

Ch	*Chondrites*
DOL	Dark-on-light
KT_{CSX}	Clayton sand body x
LOD	Light-on-dark
Ma	Mega-annum
Myr	Million years
NE	Northeast
NW	Northwest
P	*Planolites*
Pa	*Palaeophycus*
Ph	*Phycosiphon*
SW	Southwest
Ta	*Taenidium*
TAGC	Tejas A; Gulf Coast
Te	*Teichichnus*
Th	*Thalassinoides*
USGS	United States Geological Survey
WNW	West-north-west
$\overline{x}$	Average
Zo	*Zoophycos*

1. INTRODUCTION

The focus of this study is the Moscow Landing section, which refers to Upper Cretaceous and Lower Paleocene rocks exposed for approximately 1.5 km along the west bank of the Tombigbee River, Sumter County, Alabama (Fig. 1.1). This section has been the subject of considerable study owing to its spectacular exposure of the Cretaceous-Paleogene boundary and associated event(?) beds (Fig. 2.1A). Previous studies have focused on discontinuous, thin sand beds (Clayton sands; see below) that purportedly were emplaced by Cretaceous-Paleogene impact-related megawaves (Smit et al., 1996; Hart et al., 2013; Savrda, 2018).

Although the Cretaceous-Paleogene boundary deposits are relatively well-studied, the overlying Paleocene (Danian) deposits of the Clayton Formation are also well exposed but have received limited attention. These deposits include a sequence of alternating limestones and marlstones, which host unusually large and complex burrow systems, and a prominent chalk bed hereafter referred to as the Clayton chalk (Fig. 2.2B). The overarching goal of the thesis research is to improve our overall understanding of the Moscow Landing section. The study has three specific objectives: (1) to generate a detailed geologic strip map of the Moscow Landing exposure; (2) to characterize the ichnology and sedimentology of Clayton limestones and marlstones and associated large burrows; and (3) to document the sedimentology and ichnofabrics of the Clayton chalk.

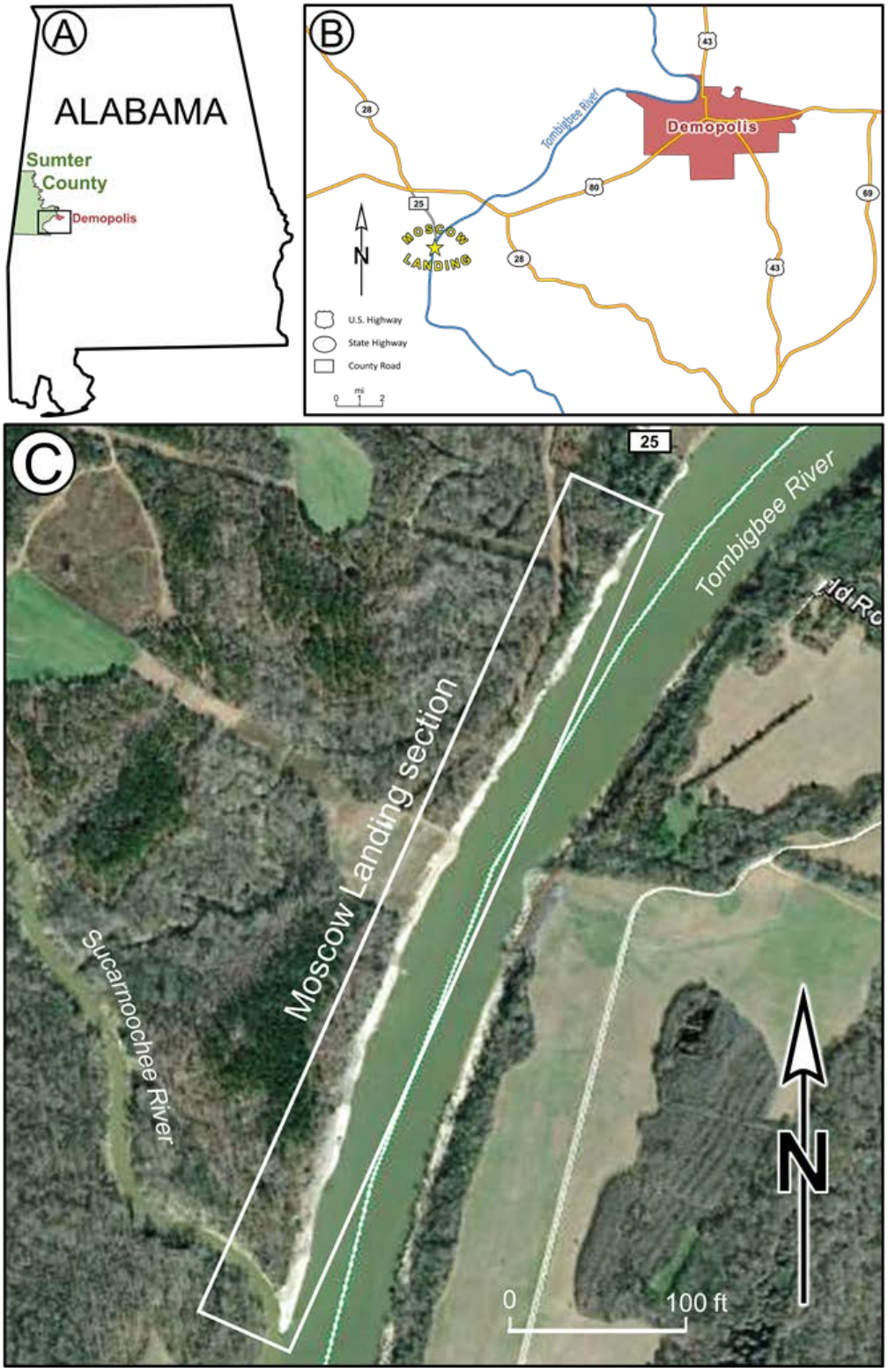

Figure 1.1 – Study location. **A**) Generalized map of Alabama showing the position of Sumter County and Demopolis. The area within the box is enlarged in B. **B**) Map showing location of the Moscow Landing section along the Tombigbee River. **C**) Google Earth aerial photograph showing the Moscow Landing exposure (white rectangle) on the west bank of the Tombigbee River (Image captured on February 15, 2015).

2. STRATIGRAPHIC CONTEXT

2.1 General Stratigraphy

The Paleocene (Danian) Clayton Formation crops out in a roughly east-west belt across Alabama (Fig. 2.1A). The Clayton Formation overlies the Upper Cretaceous Providence Sand in eastern Alabama and the Prairie Bluff Chalk in western Alabama, and it is overlain by the Paleocene Porters Creek Formation throughout most of the outcrop belt (Fig. 2.1B).

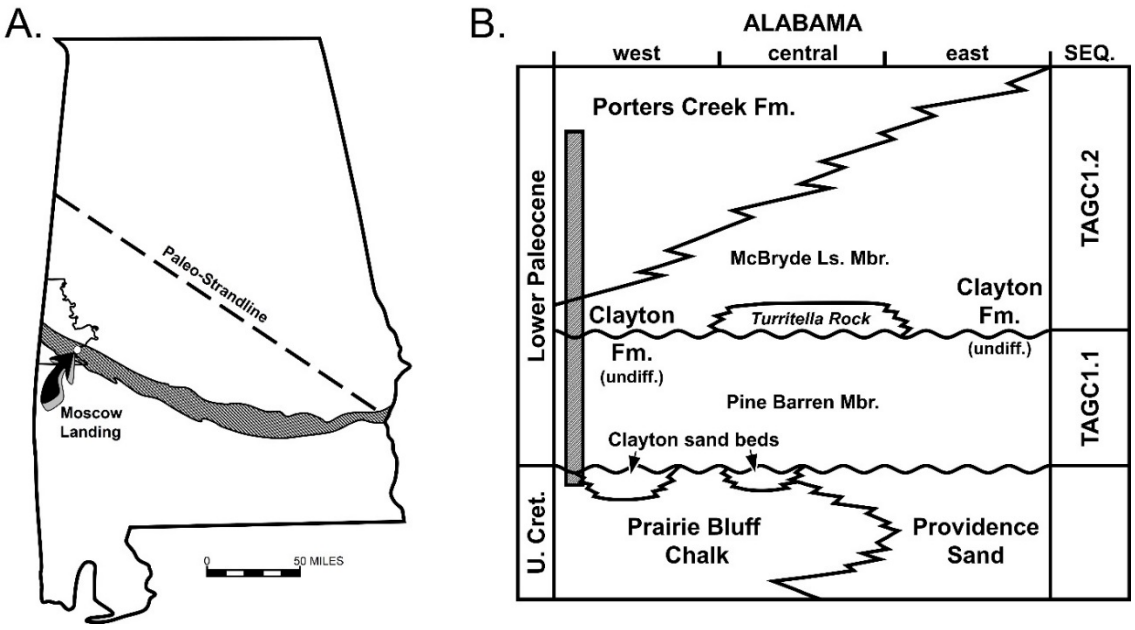

Figure 2.1 – A) Outcrop distribution of Paleocene strata (gray) in Alabama and location of the Moscow Landing section. **B**) Generalized stratigraphy of Upper Cretaceous and Lower Paleocene strata across Alabama. Shaded bar indicates strata exposed at Moscow Landing (modified from Savrda, 1991).

In central Alabama, the Clayton Formation is relatively thick (~45 m) and is divided into two members: the lower Pine Barren Member, which includes localized thin sand bodies (Clayton sands) at its base and a gastropod-rich,

sandy unit (i.e., "*Turritella* rock") at its top; and the upper McBride Member (Fig. 2.1B; Mancini and Tew, 1988; Savrda, 1991). In western Alabama, the area of the current study, the Clayton Formation is thinner (~10 m) and is not differentiated into members.

Several studies have proposed sequence stratigraphic frameworks for the Clayton Formation (Baum and Vail, 1988; Mancini and Tew, 1988, 1993; Savrda, 1991). Generally, the Clayton Formation is interpreted to comprise parts of two depositional sequences, most recently referred to as TAGC-1.1 and TAGC-1.2 (Mancini and Tew, 1993) (Fig. 2.1B). Sequence TAGC-1.1 (i.e., TP1.1 of Baum and Vail, 1988; TP1.1a of Mancini and Tew, 1988; Savrda, 1991) includes the Clayton sand bodies (variably interpreted as lowstand incised valley fills and/or impact-induced megawave deposits – compare Smith, 1997 and Smit et al., 1996) and the bulk of the Pine Barren Member (transgressive and highstand systems tracts). Sequence TAGC-1.2 (i.e., TP1.2 of Baum and Vail, 1988; TP1.1b of Mancini and Tew, 1988; Savrda, 1991) includes the "Turritella rock," the McBride Member (lowstand and transgressive systems tracts), and the basal portion of the Porters Creek Formation (highstand systems tract).

2.2 Moscow Landing Stratigraphy

Strata exposed at Moscow Landing have been described by various authors (Harrer, 1986; Mancini and Tew, 1988, 1993; Savrda, 1991; Smit et al., 1996; Smith, 1997; Hart et al., 2013; Savrda, 2018). The most detailed stratigraphic column for the Clayton Formation was prepared by Savrda (1991),

who divided the Clayton Formation and the overlying Porters Creek Formation into 25 units (Fig. 2.2).

In ascending order, the section consists of discontinuous Clayton sand bodies (units 1-3); a thin package of glauconitic sandy marls and marlstones with common *Ostrea pulaskensis* (units 4-9); a thicker sequence of marls (even-numbered units 10-24) with subordinate, thin interbeds of marly limestone (odd-numbered units 11-17 and unit 21), a glauconitic and phosphatic, sandy and pebbly limestone (unit 19), and a chalk (Clayton chalk; unit 23); and dark clays of the basal Porters Creek Formation (unit 25).

The sequence stratigraphic context of the Moscow Landing section is shown in Fig. 2.2. The basal Clayton sands (units 1-3) have been interpreted as incised valley fill deposits (Savrda, 1991; Smith, 1997) and/or megawave deposits (Smit et al., 1996; Savrda, 2018) at the base of sequence TAGC-1.1. Units 4-9 and units 10-18 represent the transgressive systems tract/condensed section and highstand systems tract, respectively, of TAGC-1.1. Unit 19, inferred to be a transgressive lag resting on the coplanar sequence boundary/transgressive surface of TAGC-1.2, is overlain by the transgressive systems tract/condensed section (units 20-23) and the highstand systems tract (units 24-25) of sequence TAGC-1.2 (Savrda, 1991).

In the current study, all exposed units (Prairie Bluff Chalk, Clayton Formation, and Porters Creek Formation) were mapped as reported in Chapter 4. The large burrow systems addressed in Chapter 5 generally correspond to the

HST of sequence TAGC-1.1. The Clayton chalk addressed in Chapter 6 represents the condensed section of sequence TAGC-1.2.

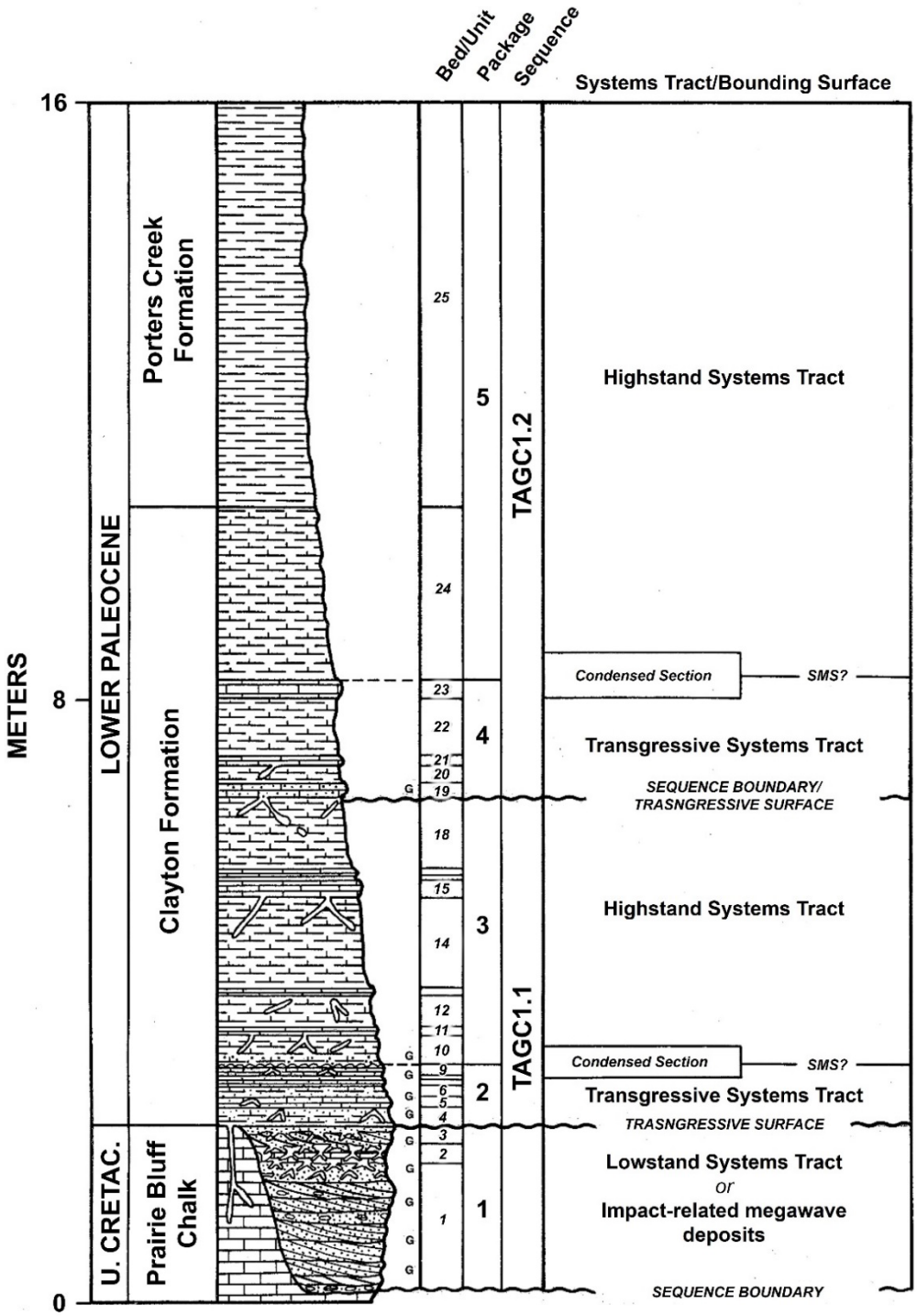

Figure 2.2 – Generalized stratigraphic column and sequence stratigraphic context of the Moscow Landing section (modified from Savrda, 1991).

3. METHODS

3.1 Objective 1 – Mapping the Moscow Landing Section

A detailed map of the Moscow Landing section was produced by tracing features observed in the field on enlarged Google Earth images. The mapped section parallels the Tombigbee River for approximately 1 mile, extending from the site of the now-defunct barge-refueling station in the north (~350 feet south of the remains of the old Rooster Bridge) southward to the Tombigbee River's confluence with the Sucarnoochee River (Fig. 2.3). Mapping of units was completed over three days (November 18-19 and December 16, 2017) when, according to the USGS (2017), the average gage height of the Tombigbee River was only ~1 ft lower than on the date of capture of the aerial photographs employed as base maps (February 15, 2015). Because of the narrow width of exposures (50-100 ft) relative to the length of the mapped shoreline, production of a single-panel map proved impractical. Instead, the map was prepared in nine partly overlapping segments or strips (Fig. 2.3), each of which encompass ~650 of shoreline length.

The map depicts the distribution and attitudes (strike and dip) of stratigraphic units and faults as measured with a Brunton compass. Units mapped are, in ascending order, the upper part of the Cretaceous Prairie Bluff Chalk, including a thin, partly phosphatic fossil-lag bed therein; six distinct,

discontinuous “Clayton sand” bodies linked to megawave deposition and/or related sea-level changes; the Paleocene Clayton Formation, including the aforementioned Clayton chalk bed (unit 23 in Fig. 2.2) in its upper part; and the lower part of the Paleocene Porters Creek Formation. Results of the mapping are presented in Chapter 4.

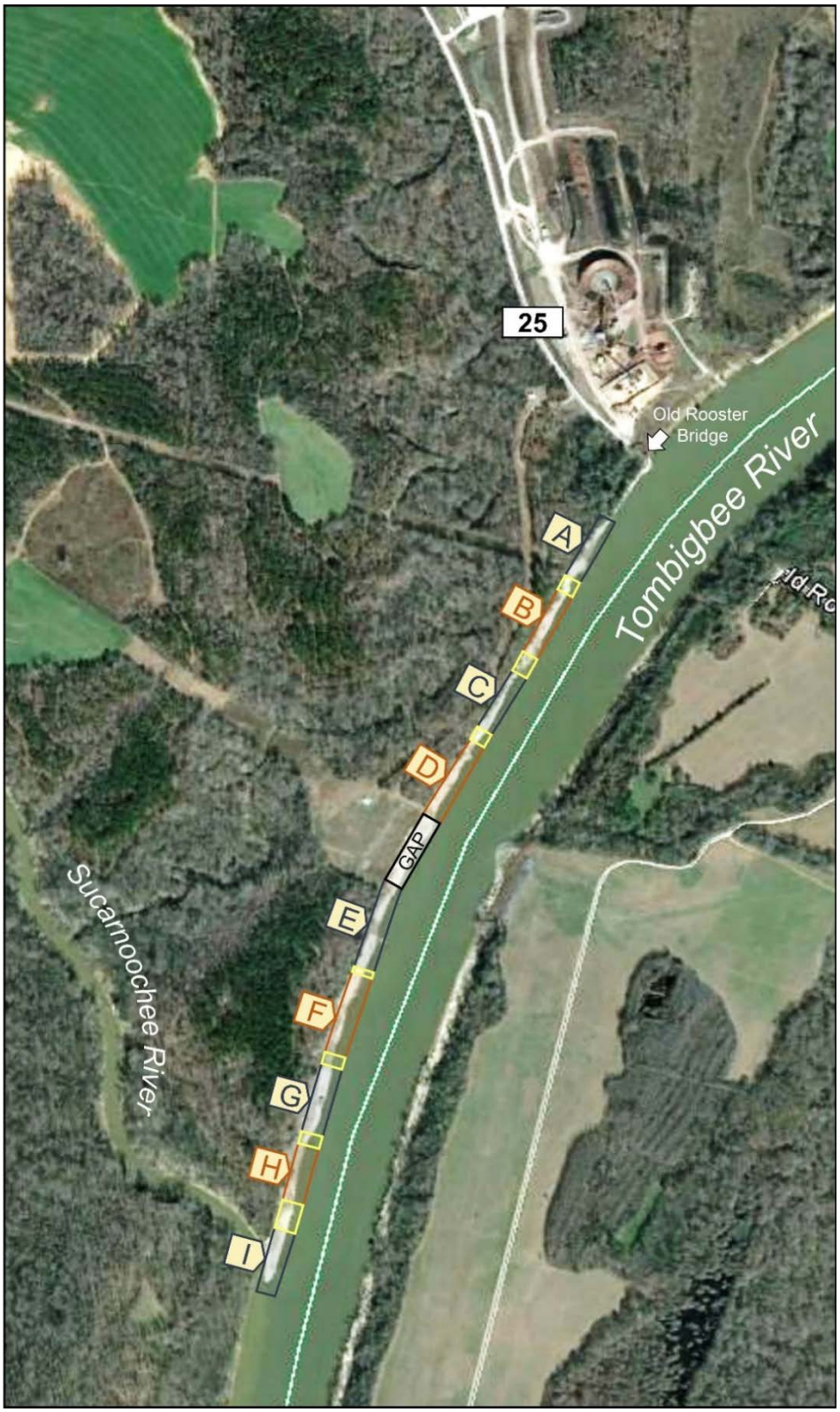

Figure 2.3 – Aerial photograph of Moscow Landing with boundaries of map segments delimited and labeled. Yellow boxes indicate areas of overlap between mapped segments A through I (Google Earth image captured on February 15, 2015).

3.2 Objective 2 – Characterization of Large Crustacean Burrow Systems

Work for objective 2 was initiated in Fall 2017 and completed in Fall 2018. After thorough reconnaissance of the Clayton Formation exposed at Moscow Landing, two stratigraphic horizons characterized by well-expressed burrow systems were identified. Burrow systems, which emanate from and are passively filled with the overlying limestone, occur within marlstones where they weather out in positive relief. Selected burrow systems from each stratigraphic horizon were carefully excavated using hand tools in an attempt to expose their three-dimensional geometry. Burrow system 1 is hosted in unit 14 marls and originated from the base of bed 15. Burrow system 2 is hosted in unit 18 marls and originated from the base of bed 19. Following the completion of excavations and field observations thereof, burrow systems were systematically photographed for more detailed morphometric analysis in the laboratory. Several block samples of host and source beds (units 14 and 18, and units 15 and 19, respectively) and selected large burrow segments were collected for sedimentologic and/or ichnologic analyses.

Block samples of the host and source beds were cut in the laboratory to produce clean vertical surfaces for detailed ichnofabric analysis, which involved evaluation of degree of bioturbation and identification of recurring ichnotaxa. Blocks also were subsampled for carbonate analysis via acid digestion and for petrographic thin-section studies of sediment composition and textures. Ichnofabrics, carbonate data, and petrographic observations of the host and source beds were integrated to evaluate the depositional conditions that

prevailed before and during the emplacement of the large burrow systems. Sampled burrow segments were carefully cleaned of mud matrix to better characterize burrow-wall features. Select burrow segments were cut and sampled for production of thin sections. Polished faces of cut burrow segments and thin sections were examined to characterize the nature of large burrow fills.

Burrow characteristics observed in this study (e.g., overall burrow system morphology, size, and depth; burrow lengths, diameters, and heights; branching frequency and angles; presence and character of wall bioglyphs; and fabric of burrow fills, etc.) were compared to those of similar large burrow systems described in previous studies (e.g., Hayasaka, 1935; Chapman and Rice, 1971; Braithwaite and Talbot, 1972; Hill and Hunter, 1973; Allen and Curran, 1974; Frey et al., 1978; Frey and Howard, 1985; Griffis and Suchanek, 1991; D'Alessandro and Bromley, 1995; Nickell and Atkinson, 1995; Gibert, 1996; Tamaki and Ueno, 1998; Schlirf, 2000; Kinoshita, 2002; Gibert and Robles, 2005; Pervesler and Hohenegger, 2006; Carvalho et al., 2007; Gibert and Ekdale, 2010; Melchor et al., 2010; Belaústegui et al., 2014; Knaust et al., 2016). Following detailed comparison, the excavated burrow systems were assigned to (an) ichnotaxon/ichnotaxa, and potential tracemakers and paleoethology were evaluated. In turn, inferences drawn from these large burrow systems were applied towards an improved understanding of paleoenvironments and sea-level dynamics during deposition of the marl-limestone interval of the Clayton Formation. Results and discussion pertaining to these large burrow systems are presented in Chapter 5.

3.3 Objective 3- Analysis of the Clayton Chalk

Work for objective 3 began in Spring 2018 and continued through Fall 2018. Field observations, including bed thickness, color, presence of sedimentary and biogenic structures, etc., were made of the Clayton chalk bed and immediately sub- and superjacent marls. Targeted sections were photographed in situ. The chalk and subjacent marls were collected in large blocks (15-20 cm wide) for detailed laboratory analysis. Block samples were collected at several locations spaced from 2 to 5 m apart.

In the laboratory, block samples were cut with a reciprocating saw and then smoothed with a shave blade to produce clean surfaces for ichnofabric studies. Ichnofabric analyses included identification of recurring ichnotaxa and the characterization of their sizes, orientations, and cross-cutting relationships. Consecutive subsamples through the marl-chalk transition were collected for carbonate analysis via acid digestion. Additional subsamples were collected for petrographic thin-section studies that allowed more detailed descriptions of sediment composition and texture, as well as of burrow morphology, burrow fills, and other relevant smaller-scale ichnologic features.

Following ichnofabric analysis of the block samples, observations made on the Clayton chalk were compared with those previously made on Cretaceous chalks in the region (e.g., Mooreville, Demopolis, and Prairie Bluff chalks; Frey and Bromley, 1985; Locklair and Savrda, 1998a; 1998b; Savrda, 2014) and elsewhere (Savrda, 2012, and references therein). Clayton chalk ichnofabrics were used to infer paleoenvironmental parameters, including substrate character,

benthic oxygenation, and relative water depth. Results of analyses of the chalk bed are presented and discussed in Chapter 6.

4. MAP OF MOSCOW LANDING

4.1 Introduction

The Moscow Landing strip map consists of nine partly overlapping segments (A-I, in Fig. 4.1). In addition to manmade landmarks (e.g., powerlines, gas line riprap), the map depicts the distribution of the upper part of the Prairie Bluff Chalk (K_{pc}) and its component prominent fossil marker bed; Clayton sand bodies ($KT_{cs1\text{-}cs6}$); the Clayton Formation (TP_c), including its prominent chalk marker bed; the lower part of the Porters Creek Formation (TP_p); and associated structural features (e.g., faults). Stratigraphic units and structural features are described below in sections 4.2 and 4.3, respectively.

4.2 Stratigraphic Units

4.2.1 Prairie Bluff Chalk

The upper part (up to 4 m, depending on the river level) of the Maastrichtian Prairie Bluff Chalk is exposed in the northern part of the map area (K_{pc} in map panels A-D; Fig. 4.1). The Prairie Bluff here comprises dm- to m-scale rhythmically interbedded light and medium gray, moderately indurated, heavily bioturbated, sparsely to highly fossiliferous, micaceous, variably glauconitic, sandy chalks and marlstones and a prominent fossil-lag bed (Fig. 4.2A). Ichnofossils in the chalk include *Thalassinoides*, *Chondrites*, and *Cylindrichnus* (Fig. 4.2B). The fossil-lag bed includes *Entobia*-bored *Exogyra* shells and phosphatized steinkerns of gastropod, pelecypod, and cephalopod

Figure 4.1 Geologic strip map of Moscow Landing section generated in the field employing Google Earth photographic imagery dated 2/15/15. Note variable overlap between map panels.

(ammonoids and nautiloids) molluscs (Fig. 4.2C). This mapped marker bed typically lies approximately 1.5 m below the top of the Prairie Bluff Chalk. However, it is locally truncated at the base of Clayton sand bodies (e.g., KT_{cs3} in map panel B, Fig. 4.1) or the base of the Clayton Formation (TP_c in map panel D, Fig. 4.1; Fig. 4.2D).

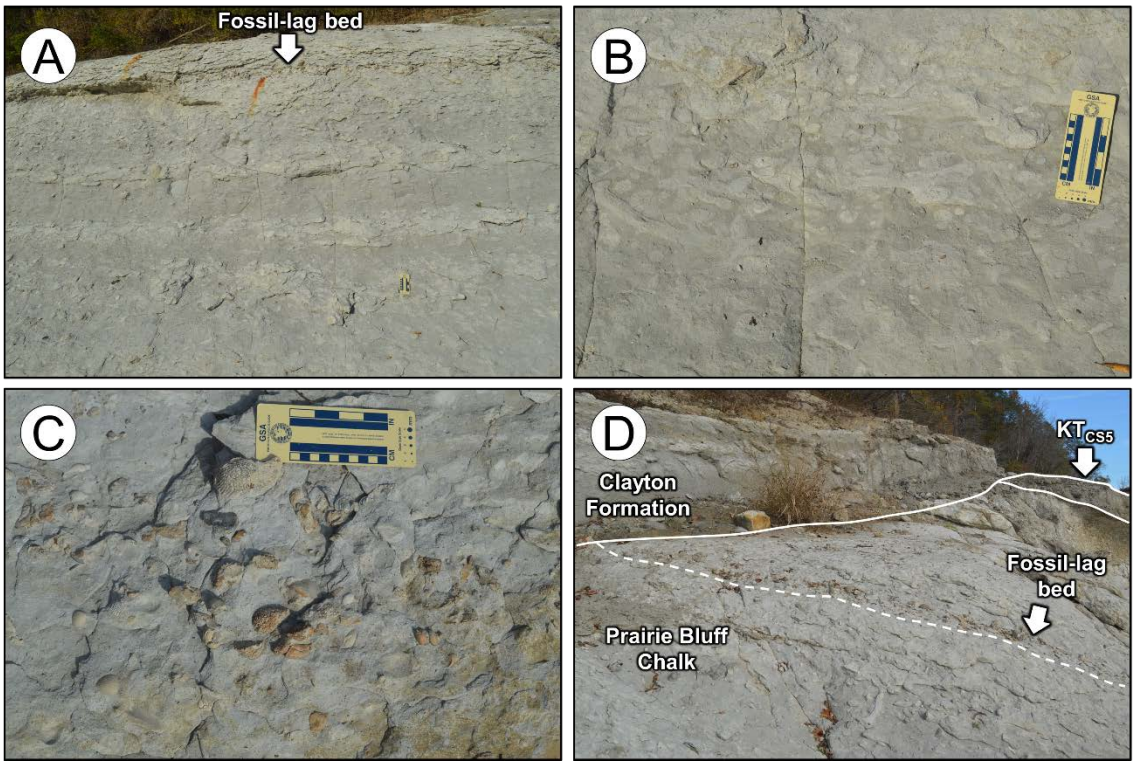

Figure 4.2 – Prairie Bluff Chalk. **A**) The upper part of the Prairie Bluff Chalk exposed at Moscow Landing (the fossil-lag bed is labeled with an arrow). **B**) *Thalassinoides*-dominated ichnofabric in Prairie Bluff Chalk. **C**) Close-up photograph of the fossil-lag bed. **D**) Fossil-lag bed locally truncated at base of Clayton Formation.

4.2.2 Clayton Sand Bodies

Six distinct, discontinuous Clayton sand bodies occur in the northern part of the mapped section (KT_{cs1}-KT_{cs6} in map panels A-E; Fig. 4.1). These sand bodies, which range in thickness from 0 to 2 m, are dominated by grayish orange, moderately indurated, sparsely fossiliferous, locally bioturbated, planar to wavy laminated or massive, poorly sorted, medium- to coarse-grained, calcite-cemented sandstone (Fig. 4.3A, B) with localized concentrations of reworked Cretaceous fossils (e.g., *Exogyra*) and clasts of Prairie Bluff Chalk. The latter locally form breccias, up to 1.5 m thick, along sand-body bases or near fault-bounded sand-body margins (e.g., Fig. 4.3C).

Bases of sand bodies truncate stratification in the underlying Prairie Bluff Chalk, including the fossil-lag bed therein. As previously noted by Smit et al. (1996), the geometry of Clayton sand bodies is highly variable. Some sand bodies appear to form nearly symmetrical, channel-form masses (e.g., KT_{cs1} and KT_{cs4}, map panels A and C, respectively; Fig. 4.1; Fig. 4.3D). However, others are fault bounded at one or both termini and are markedly asymmetric. For example, sand body KT_{cs3} increases in thickness southward before it terminates against and is deformed along north-dipping normal faults (Fig. 4.3E). In all cases, tops of Clayton sand bodies are erosionally truncated at the base of the superjacent Clayton Formation. Bioturbation of Clayton sand bodies is generally limited to the uppermost decimeter wherein well-developed *Thalassinoides* burrow systems extend downward from the base of the Clayton Formation (Fig. 4.3F). However, some sand bodies (e.g., KT_{cs1} and KT_{cs5}) may contain internal bioturbated horizons, as recently noted by Savrda (2018).

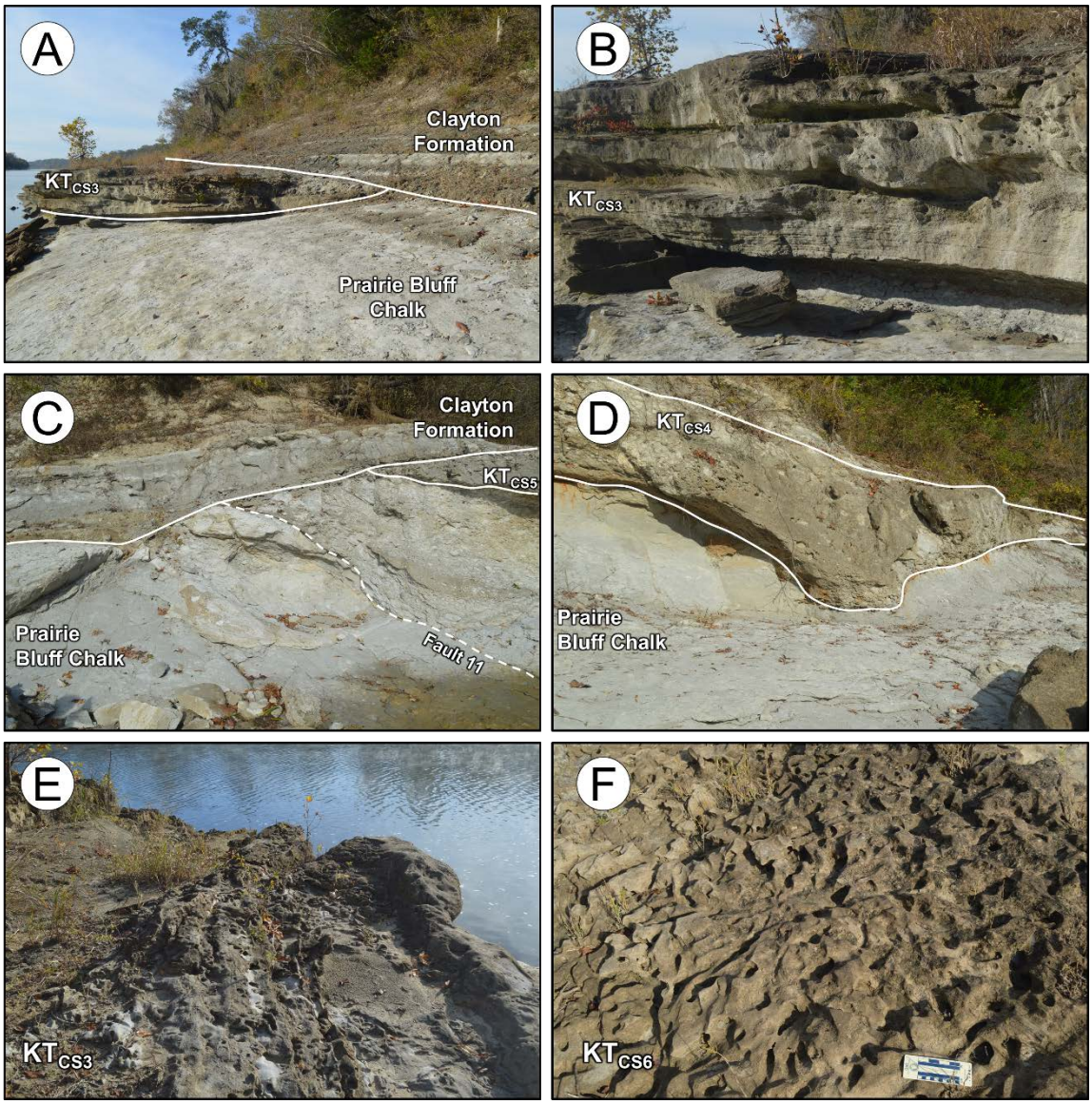

Figure 4.3 – Clayton sand bodies. **A**) South-facing photograph of the top of the Prairie Bluff Chalk, a discontinuous Clayton sand body, and the lower part of the Clayton Formation. **B**) Close-up photograph of KT_{cs3}. **C**) Prairie Bluff Chalk pebble and cobble breccia near a fault-bounded sand-body margin. **D**) Nearly symmetrical channel-form Clayton sand body. **E**) Near vertical parallel-laminated sand beds at fault-bounded southern terminus of Clayton sand body KT_{cs3}. Note disruption of sandstone by horizontal *Thalassinoides* burrow systems penetrating from the base of the overlying Clayton strata. **F**) Well-developed *Thalassinoides* burrow systems at the top of KT_{cs6}.

4.2.3 Clayton Formation

Parts of the ~8-m-thick Clayton Formation are exposed along the entire mapped section (TP_c in Fig. 4.1). The basal part of this unit is a 1-to-2-m-thick interval of very sandy glauconitic marlstones and sandy, glauconitic micritic limestones containing abundant small shells of *Ostrea pulaskensis* (Fig. 4.4A, B; units 4-9 in Fig. 2.2). The remainder of the unit (~6 m thick) is dominated by relatively thick (18-120 cm), dark olive-gray, poorly indurated marls but also includes relatively thin (9-32 cm), better indurated, more carbonate-rich interbeds (Fig. 4.4A; units 10-24 in Fig. 2.2). The carbonate-rich intervals include, in ascending order, several marly limestone beds that are the source horizons for the large burrows described in Chapter 5 (units 11, 13, 15, 17 in Fig. 2.2); a glauconitic limestone bed with common dark phosphate pebbles (unit 19 in Fig. 2.2); and a distinctive chalk bed (unit 23 in Fig. 2.2, see Chapter 6). Despite local offsets by faults, all of these relatively resistant units can be traced laterally within the map area. However, only the position of the Clayton chalk bed (unit 23) is depicted on the map (Fig. 4.1).

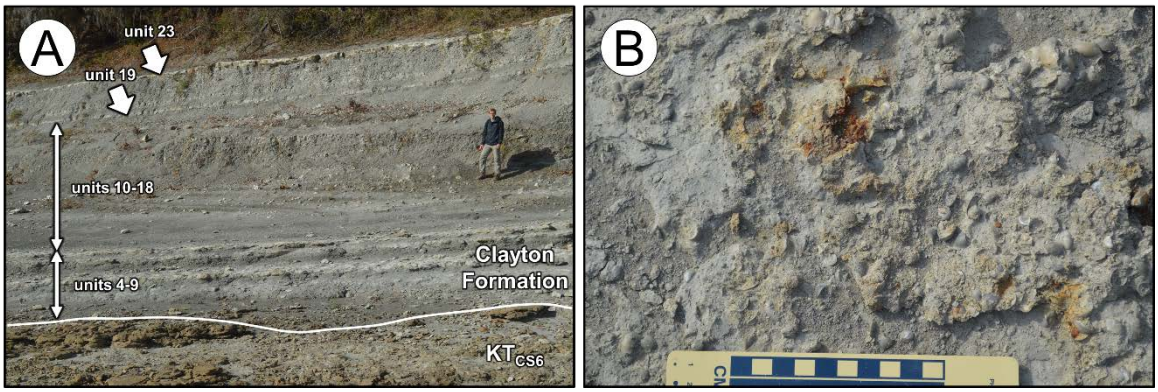

Figure 4.4 – Clayton Formation. **A**) Photograph of the Clayton Formation (units 4-23). **B**) Close-up photograph of the lower part of the Clayton Formation containing abundant shells of *Ostrea pulaskensis* (top of unit 9).

4.2.4 Porters Creek Formation

The lower parts of Porters Creek Formation, up ~6 m thick, are exposed only in the southern half of the map area (TP_p in panels E-I, Fig. 4.1), reflecting the southerly regional dip of coastal plain strata. The Porters Creek Formation exposed at Moscow Landing consists of olive-black, massive to weakly bioturbated, carbonaceous, slightly calcareous clay (Fig. 4.5). Where visible, trace fossils include *Chondrites* and small *Planolites*. Although the clay contains few macrofossils, well-preserved benthic foraminifera are readily apparent in hand lens.

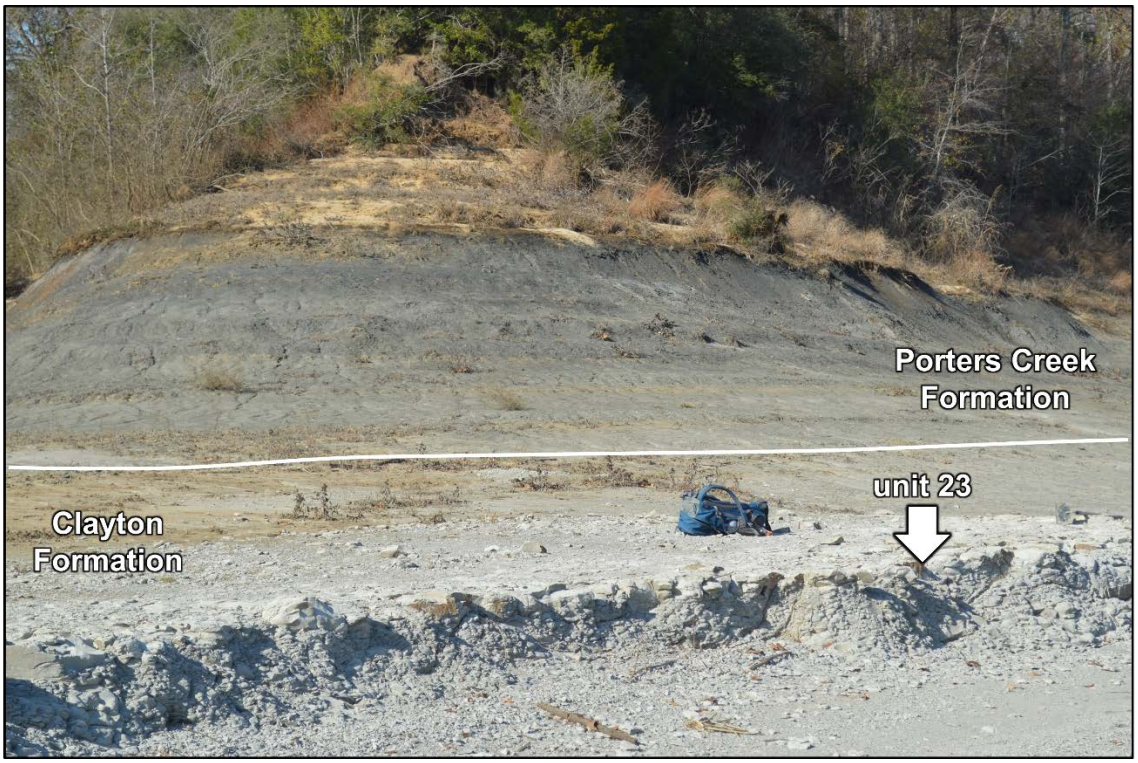

Figure 4.5 – Photograph of the upper part of the Clayton Formation and basal part of the Porters Creek Formation at the southern end of the Moscow Landing exposure. The prominent chalk bed of the Clayton Formation (unit 23) can be seen in the lower part of the photograph.

4.3 Structural Features

Twenty-two (22) faults, labeled 1 through 22 in order of appearance from north to south, are recognized at the Moscow Landing section (Fig. 4.1; Table 4.1). These faults can be divided into two groups: type 1 and type 2 faults. Type 1 faults offset Cretaceous strata but are truncated at the base of the Clayton Formation, indicating that displacement occurred at or near the Cretaceous-Paleocene transition. In contrast, type 2 faults offset all Cretaceous and Paleocene units, indicating later deformation. However, based on the disposition and character of associated Clayton sand bodies, some type 2 faults likely were active contemporaneous with type 1 faults and then were later reactivated.

With several exceptions, type 1 and 2 faults generally strike west-northwest. With the exception of six southerly dipping faults, four of which occur in the southern part of the map area, faults generally dip to the NE or NW at 35 to 60 degrees (Table 4.1). Virtually all faults reflect normal displacement, although well-developed slickensides on some surfaces reflect a minor oblique component.

Table 4.1 – Type and attitude of faults recognized at Moscow Landing.

Fault #	Type	Strike	Dip angle
1	1	N07E	58NW
2	1	No data	No data
3	1	N87E	50NW
4	2	N86W	47NE
5	1	N88W	45NE
6	1	N55W	35SW
7	1	N87E	40NW
8	2	N53W	55NE
9	1	N45W	59 SW
10	1	No data	No data
11	1	No data	No data
12	2	N85E	66NW
13	2	E-W	60N
14	2	No data	No data
15	2	N82W	56NE
16	2	N43W	35SW
17	2	N77W	40SW
18	2	N70W	40NE
19	2	N20W	49SW
20	2	No data	No data
21	2	No data	No data
22	2	N52E	70SE

The gentle southerly regional dip (<1 to 9 degrees) characteristic of Coastal Plain strata is manifested in southward younging and (sparse) strike-and-dip data mainly derived from bedding surfaces in the Clayton Formation (Fig. 4.1). However, oversteepening caused by drag is observed along some faults, and reversals in dip direction are observed locally, reflecting very gentle warping. Very broad synclinal or anticlinal structures are developed above some fault-bounded Clayton sand bodies (e.g., KT_{cs2}, map panel A, and KT_{cs5}, map panel D, respectively, in Fig. 4.1). Rare steep dips (up to 70 degrees) are observed only

within parts of some Clayton bodies where bedding has been distorted adjacent to faults (e.g., southern terminus of KT_{cs3}, map panel B, Fig. 4.2, 4.3E).

4.4 Relation to Other Current Studies

Studies of large branching networks focused on exposed burrows of the Clayton Formation, mainly those in the southern part of the map area (map panels F-I). The main burrow excavation sites described in Chapter 5 occur in map panel G. Studies of the Clayton chalk bed described in Chapter 6 focus on outcrops at the southernmost end of the map area (map panels H-I) where both vertical and bedding-parallel surfaces of this unit are relatively fresh (i.e., less impacted by pedogenesis).

5. CLAYTON LIMESTONE/MARLSTONE RHYTHMS AND ASSOCIATED LARGE BURROW SYSTEMS

5.1 Introduction

As noted in the methods section (section 3.2), the Clayton Formation exposed at Moscow Landing features an ~4-m-thick interval (units 10-21) characterized by relatively thick (18-120 cm), dark olive gray, poorly indurated marls (49-62% $CaCO_3$) and thin (9-32 cm), light gray, indurated, locally glauconitic interbeds of marly limestone (75-86% $CaCO_3$). At least 5 sets of these marl-limestone couplets are exposed in this section (Fig. 5.1B). The marls host large, highly irregular, branching burrow systems that are preserved in full relief. These burrow systems emanate from and were passively filled with sediment derived from overlying limestones. The objective of this chapter is to characterize these large burrow systems in their sedimentologic context in an effort to assess ichnotaxonomic affinities, behavioral significance, and paleoenvironmental implications.

Observations focused on a stretch of the exposure wherein the upper marl-limestone interval is best exposed (Fig. 5.1A) and emphasized bed couplets 14-15 and 18-19 (Fig. 5.1B, C). However, additional observations were made of similar burrow systems expressed within lower marl beds.

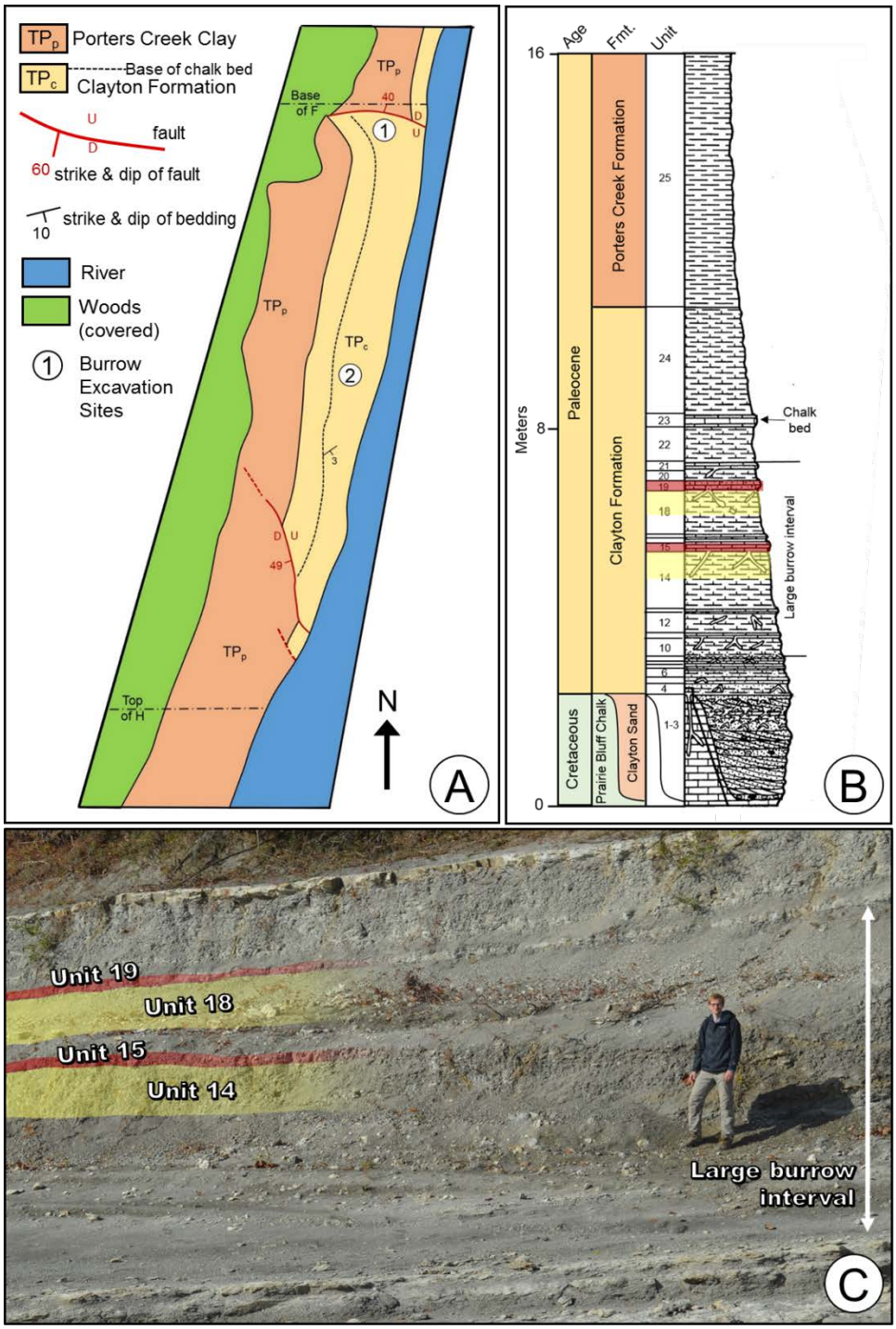

Figure 5.1 – Location and stratigraphic context of large burrow systems. **A**) Map of a portion of Moscow Landing exposure showing location of main burrow excavation sites (1, 2). **B**) Stratigraphic column depicting strata exposed at Moscow Landing. Source limestone beds for excavated burrow systems are highlighted in red and associated host marl beds are highlighted in yellow (modified from Savrda, 1991). **C**) Photograph of Clayton Formation showing marl and limestone interval containing large burrows. Marls and limestone source beds emphasized in this study are highlighted in yellow and red, respectively.

5.2 Description of the Bed Couplets

5.2.1 Bed Couplet 14-15

Bed couplet 14-15 comprises a 120-cm-thick, dark olive gray marl (Fig. 5.2A) and a 32-cm-thick, relatively resistant, light gray limestone (Fig. 5.2C). The limestone forms a subtle ledge above the less resistant marl. The $CaCO_3$ contents of the marl and limestone range from 60.94% to 62.43% ($\bar{x}$ = 61.93%, n=3) and 75.53% to 86.37% ($\bar{x}$ = 82.23%, n=3), respectively (Table 5.1).

Both the marl and limestone are completely bioturbated (Fig. 5.2A, C). Faint, lighter gray *Chondrites* are the only discrete ichnofossils observed in the marl (Fig. 5.2A). *Chondrites* are superimposed on a diffusely burrow-mottled background. Ichnofabrics of the limestone are similar; small, lighter gray structures resembling *Chondrites* overprint a homogeneous to burrow-mottled background fabric (Fig. 5.2C).

As viewed in thin section, the marl can be classified as an argillaceous sparse biomicrite (Fig. 5.2B). Skeletal allochems include abundant foraminifera and sparse mollusk fragments. Minor constituents include silt-sized quartz (<5%), pyrite (<5%), and very rare glauconite grains (<1%) and phosphatic peloids (<1%).

As viewed in thin section, the limestone can be classified as a locally microsparitic sparse biomicrite (Fig. 5.2D). Skeletal allochems include abundant foraminifera and sparse mollusk fragments. Minor components include very rare phosphatic peloids (<1%) and silt-sized quartz grains (<1%).

Table 5.1 – Range and average carbonate contents of units 14, 15, 18, and 19 based on weight loss after acid digestion in HCl.

Sample	Carbonate %	$\bar{x}$ Carbonate %
Unit 14 marl	60.94	61.93
	62.42	
	62.43	
Unit 15 limestone	75.53	82.23
	84.78	
	86.37	
Unit 18 marl	49.37	51.41
	51.91	
	52.98	
Unit 19 limestone	77.03	78.45
	77.96	
	80.35	

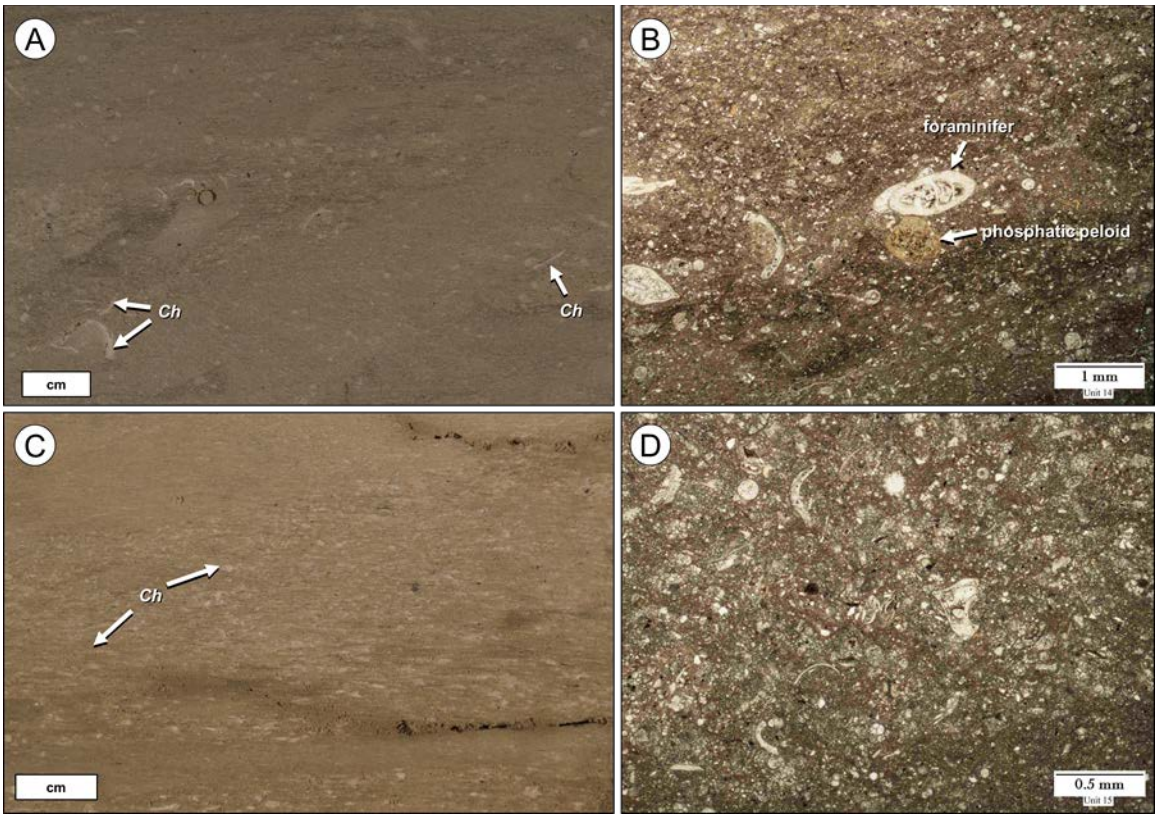

Figure 5.2 – Photographs and photomicrographs of unit 14 marl (**A**, **B**) and unit 15 limestone (**C**, **D**). **A**) Background ichnofabric of unit 14 marl (*Ch* = *Chondrites*). **B**) Photomicrograph of unit 14 marl. **C**) Background ichnofabric of unit 15 limestone (*Ch* = *Chondrites*). **D**) Photomicrograph of unit 15 limestone.

5.2.2 Bed Couplet 18-19

Bed couplet 18-19 comprises a 95-cm-thick, dark olive gray marl (Fig. 5.3A) and a 20-cm-thick, relatively resistant, light gray limestone (Fig. 5.3C). Similar to unit 15 limestone, unit 19 limestone forms a ledge above the less resistant marls of unit 18. $CaCO_3$ contents of the marl and limestone range from 49.37% to 52.98% ($\bar{x}$ = 51.41%, n=3) and 77.03% to 80.35% ($\bar{x}$ = 78.45%, n=3), respectively (Table 5.1).

The marl is heavily bioturbated (Fig. 5.3C). Ichnofabrics are dominated by relatively distinct burrows of variable size superimposed on a homogeneous to burrow-mottled background. Larger burrows likely represent cross sections of *Thalassinoides* and *Planolites*, whereas smaller, more poorly defined burrows may be *Chondrites*. The limestone also is completely bioturbated, but ichnofossils are less distinct. The presence of *Thalassinoides* is manifest in variations in the concentrations of darker glauconitic grains (Fig. 5.3C).

As viewed in thin section, unit 18 marl can be classified as an argillaceous sparse biomicrite (Fig. 5.3B). Skeletal allochems include abundant foraminifera. Subordinate components include minor quartz silt (<5%) and very rare glauconite grains (<1%) and phosphatic peloids (<1%). Bands of lighter- and darker-colored, argillaceous micrite are seen throughout the thin section (Fig. 5.3B). These bands may reflect the contrast between burrow fills and the background ichnofabrics.

As viewed in thin section, unit 19 limestone can be classified as a glauconitic and phosphatic, sparse biomicrite (Fig. 5.3D). Skeletal allochems,

including abundant foraminifera, are abundant. Sand-sized glauconite grains are common (~20%), as are sand- to fine pebble-sized (1-6 mm) phosphatic grains (~5%).

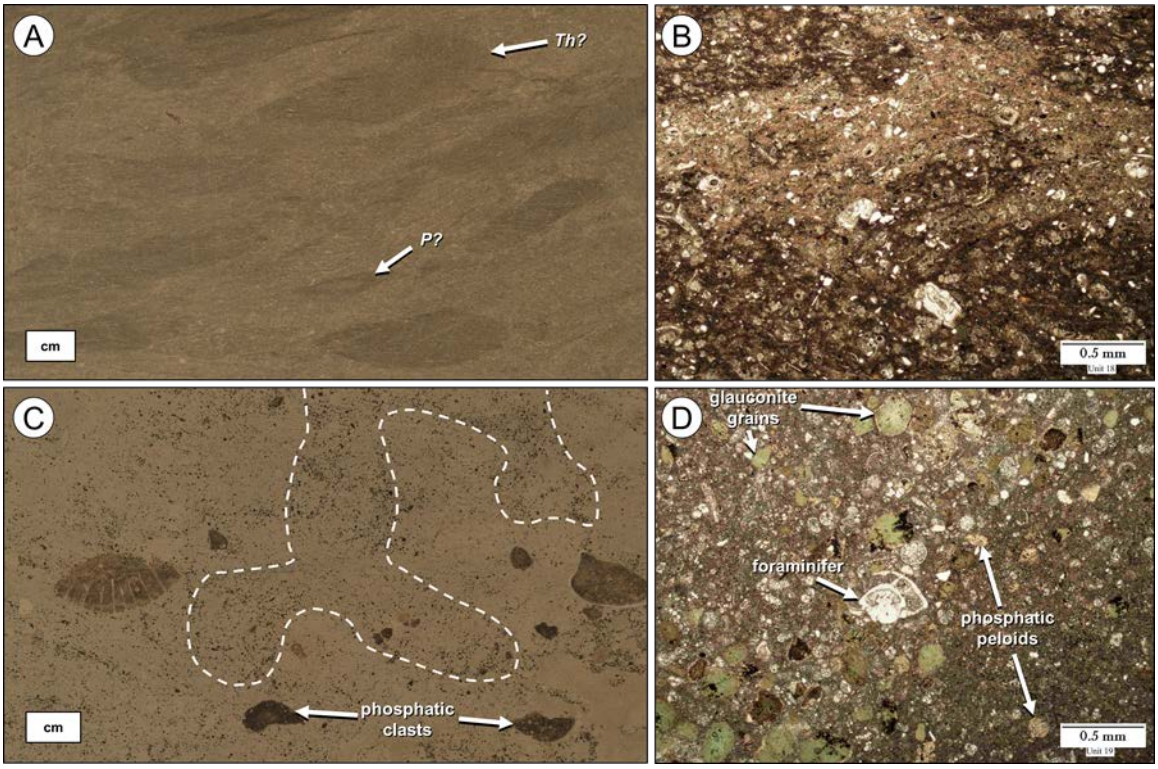

Figure 5.3 – Photographs and photomicrographs of unit 18 marl (**A**, **B**) and unit 19 limestone (**C**, **D**). **A**) Background ichnofabric of unit 18 marl (*Th?* = *Thalassinoides?*, *P?* = *Planolites?*). **B**) Photomicrograph of unit 18 marl. **C**) Background ichnofabric of unit 19 limestone. Dashed line outlines poorly defined, large branching burrows representing *Thalassinoides*. **D**) Photomicrograph of unit 19 limestone.

5.3 Description of Large Burrow Systems

5.3.1 General Description of Burrow Excavations

Burrow system 1, differentially weathering out of bed 14, was excavated in a gently sloping exposure located ~750 ft (~230 m) south of Clayton sand body 6. Burrow system 2, weathering out of unit 18, was excavated ~200 ft (~61 m) south of burrow system 1 (fig. 5.1A). Notably, neither of these burrow systems can be regarded as complete. Their spatial confines could not be fully established owing to surface weathering and erosion, which truncated burrow systems in the downslope direction, and thickness of overburden, which limited the ability to fully excavate systems in the upslope direction (Fig. 5.4). Burrow system 1 experienced a greater degree of pre-excavation erosion and was less complete; large portions of what was likely a contiguous system were missing. Overburden was more easily removed from burrow system 2, and, hence, the excavated portion of this system was more areally extensive and more complete (Fig. 5.4). The character of burrows systems 1 and 2 are described separately below.

5.3.2 Burrow System 1

A map and representative photographs of burrow system 1 are provided in figures 5.5 and 5.6. The excavation area is ~4.5 m long and ~1 m wide; its long axis trends ~N30W, perpendicular to the local slope of the outcrop. Virtually all preserved burrow segments in the excavation area lie in the same bedding-parallel horizon, which lies ~60 cm below the base of the limestone source bed

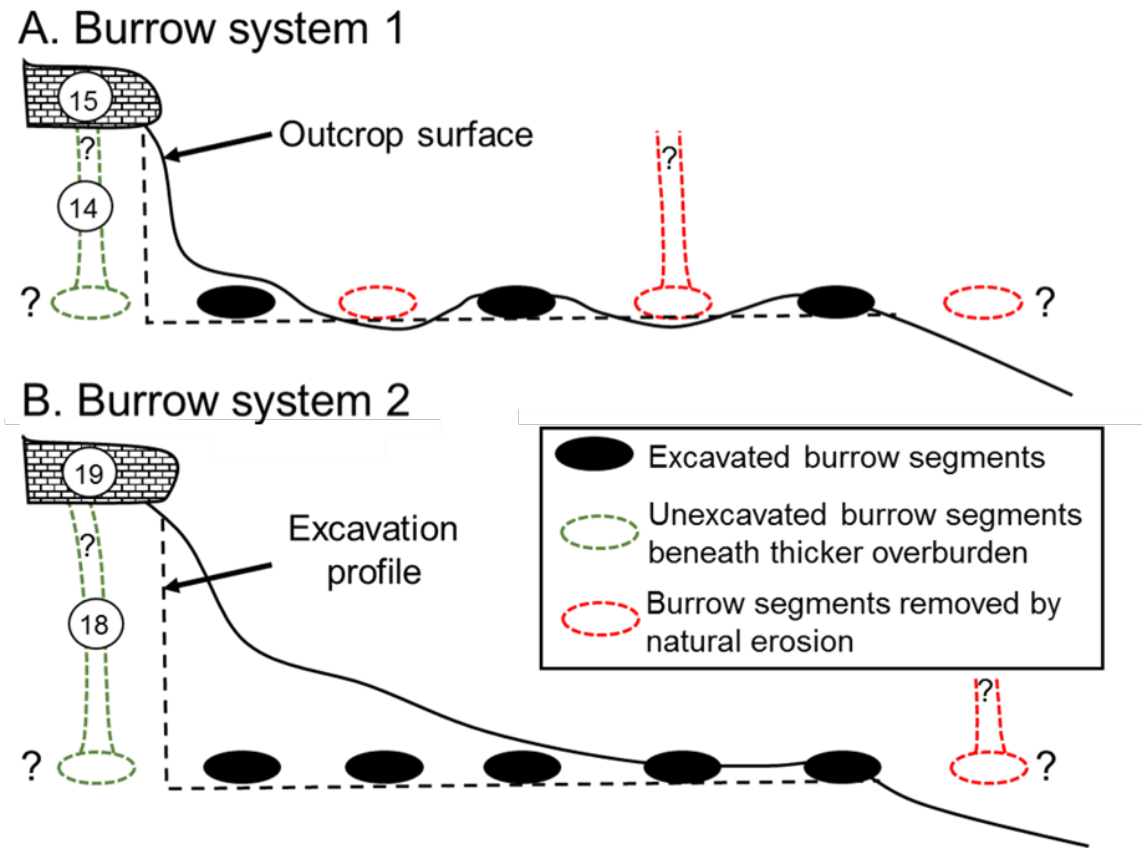

Figure 5.4 – Schematic representation depicting the relative completeness of excavated burrow system 1 (**A**) and burrow system 2 (**B**) in beds 14 and 18, respectively.

(bed 15). All segments represent what were horizontal to gently inclined tunnels. Vertical or subvertical shafts that provided connection between the horizontal burrow segments and their source horizon were not observed. Connecting shafts either existed outside of the excavation area or were connected to missing burrow segments (i.e., those that were eroded from the area prior to excavation; Fig. 5.4).

The overall morphology of this burrow system is difficult to assess owing to limited area and depth of excavation and low degree of completeness. However, the preserved and exposed parts of this system may be described as an irregularly branching maze wherein axial traces, lengths, and diameters of branches, as well as angles of branching, are variable. Individual branch segments range in length from 19 to 48 cm and are typically straight to gently curved (Figs. 5.5, 5.6), although some longer segments follow an open sinusoidal path (Fig. 5.6B). Branch bifurcation angles vary from 58 to 90 degrees; i.e., both Y- and T-shaped branch junctures occur. Burrow cross sections are generally elliptical with burrow width/height ratios ranging from 1.2 to 1.6. Burrow widths within this system range from 3 to 5 cm.

Sediments filling the tunnels of burrow system 1 were derived from and thus are similar to that of the overlying limestone (unit 15). Burrow fills lack any physical structure (e.g., lamination, grading) but commonly are cross cut by smaller burrows (*Planolites*, *Chondrites*?). The latter burrows locally conform to and are manifest on the exteriors of burrow fills, suggesting that movement of secondary bioturbators was restricted to the infilled interiors of the large burrows

(e.g., Fig. 5.6D, E). Except where smaller burrows are manifest on burrow exteriors, burrow walls are sharp and predominantly smooth; scratch marks or other bioglyphs that could be attributed to the producers of the large burrows are not apparent through the bulk of the preserved burrow system.

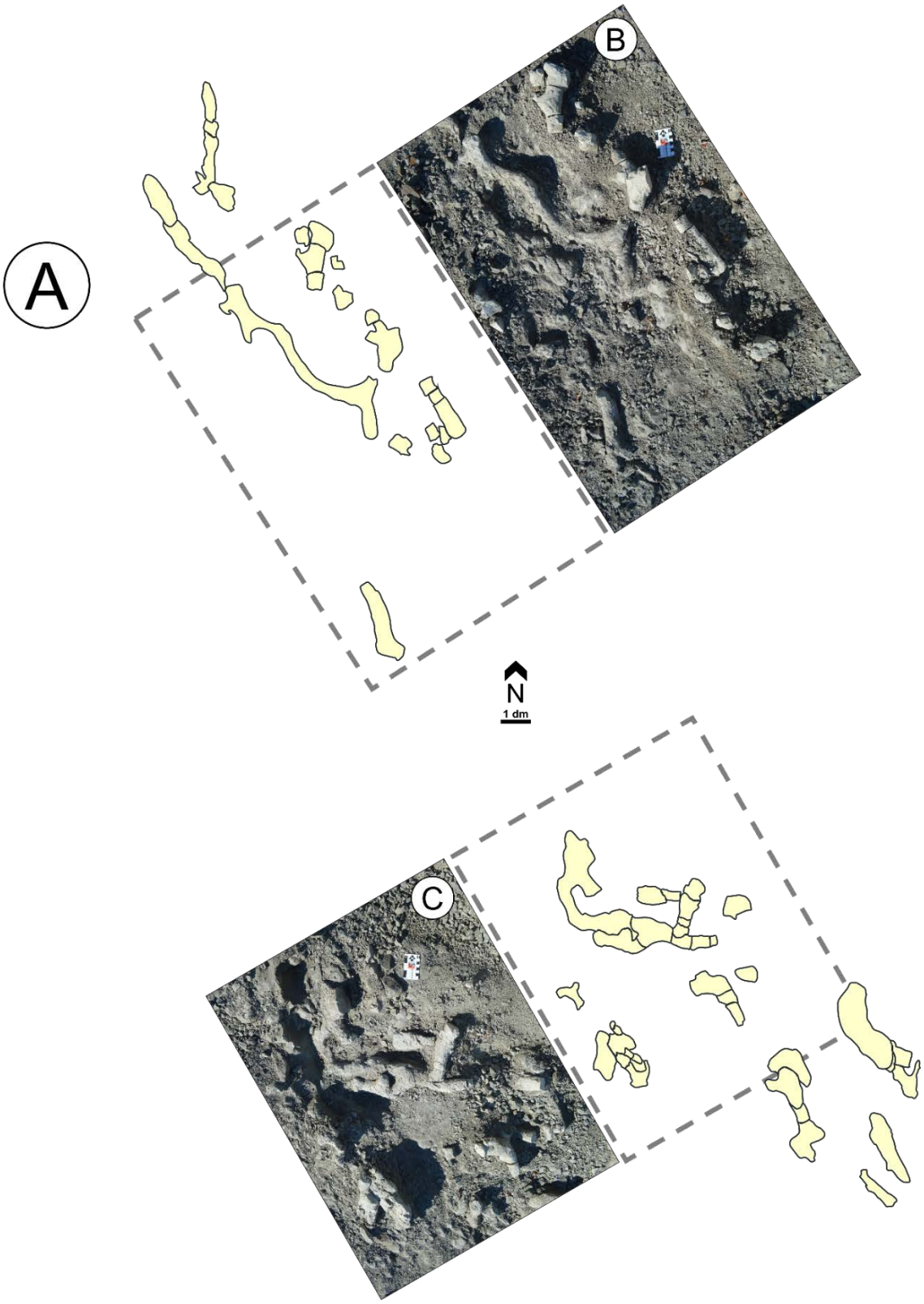

Figure 5.5 – Sketch of burrow system 1 excavation (**A**) and representative photographs of parts of the burrow system (**B**, **C**).

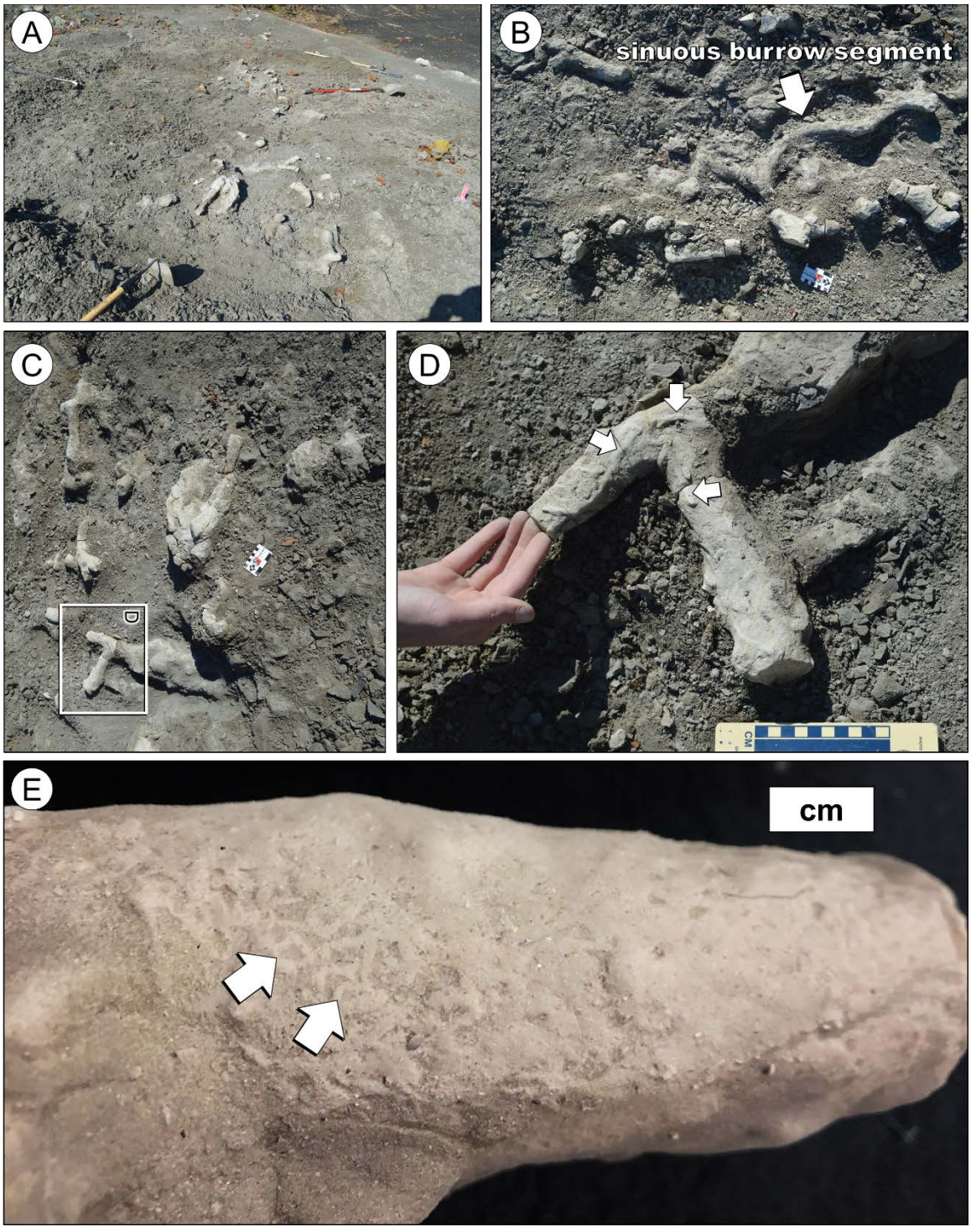

Figure 5.6 – Representative photographs of burrow system 1. **A**) Oblique photograph of entire excavated system looking towards the northwest. **B**) Photograph of northern part of system, which includes a rare sinuous burrow segment. **C**) Photograph of southern part of burrow system. Close-up of area in box is shown in D. **D**) Close-up photograph of Y-shaped branching. Note manifestation of lighter, smaller diameter burrows (*Planolites*?, arrows) along burrow walls. **E**) Photograph of small, ill-defined branching burrows (*Chondrites*?, e.g., arrows) on burrow exterior.

5.3.3 Burrow System 2

A map and representative photographs of burrow system 2 are provided in figures 5.7 and 5.8. The exposed part of this burrow system covers an area of ~5 m^2. Like burrow system 1, this more complete system is a highly irregular, branched maze consisting of predominantly horizontal burrows segments. All burrow segments lie within the same bedding-parallel horizon in unit 18 marl (Fig. 5.7), approximately ~50 cm below the base of unit 19 from which the burrows derive. Despite the relatively high degree of completeness of this burrow system, no vertical or subvertical shafts were encountered during the excavation. Again, connecting shafts either existed outside of the excavation area or were connected to missing burrow segments (Fig. 5.4).

This burrow system comprises irregularly interconnected tunnels that vary with respect to length, width, and intersection. Individual burrow segments are typically straight to gently curved, range from 21 to 87 cm in length, and exhibit elliptical cross sections with burrow width/height ratios varying from 1.2 to 1.6. Burrow width varies from 1 to 6 cm. Bifurcation angles between wider burrow segments range from 30 to 90° (Figs. 5.7, 5.8A-C), although relationships between burrow segments are typically more complex. Some parts of the system include two to three closely-spaced, vertically stacked or laterally adjacent, parallel to subparallel tunnels of similar or disparate widths that locally interconnect and cross one another in the horizontal or vertical plane; i.e., burrows segments are anastomosing or entwined (e.g., Figs. 5.7A, B, 5.8A, C). In addition, some burrow segments are characterized at their bases by short, subhorizontal, acutely to bluntly terminating blind tunnels (Fig., 5.8D, E).

Burrows in this system are filled with sandy glauconitic limestone derived from unit 19. Transverse views of burrow segments reveal that some burrow fills were preferentially re-burrowed (Fig. 5.8F). Physical structures are generally absent within fills, although grading is apparent where glauconite, fish debris(?), and possibly plant-derived organic matter is concentrated in the floors of some blind tunnels (Fig. 5.8E).

Burrow walls in this system are sharp and typically characterized by low-relief scratch traces <1 mm in width and several mm in length (Fig. 5.9A, B, C). These bioglyphs generally form rhombohedral patterns on main burrow segments (Fig. 5.9A, B) as well as on the walls of blind tunnels. However, transverse bioglyphs are locally manifest on burrow floors (Fig. 5.9C).

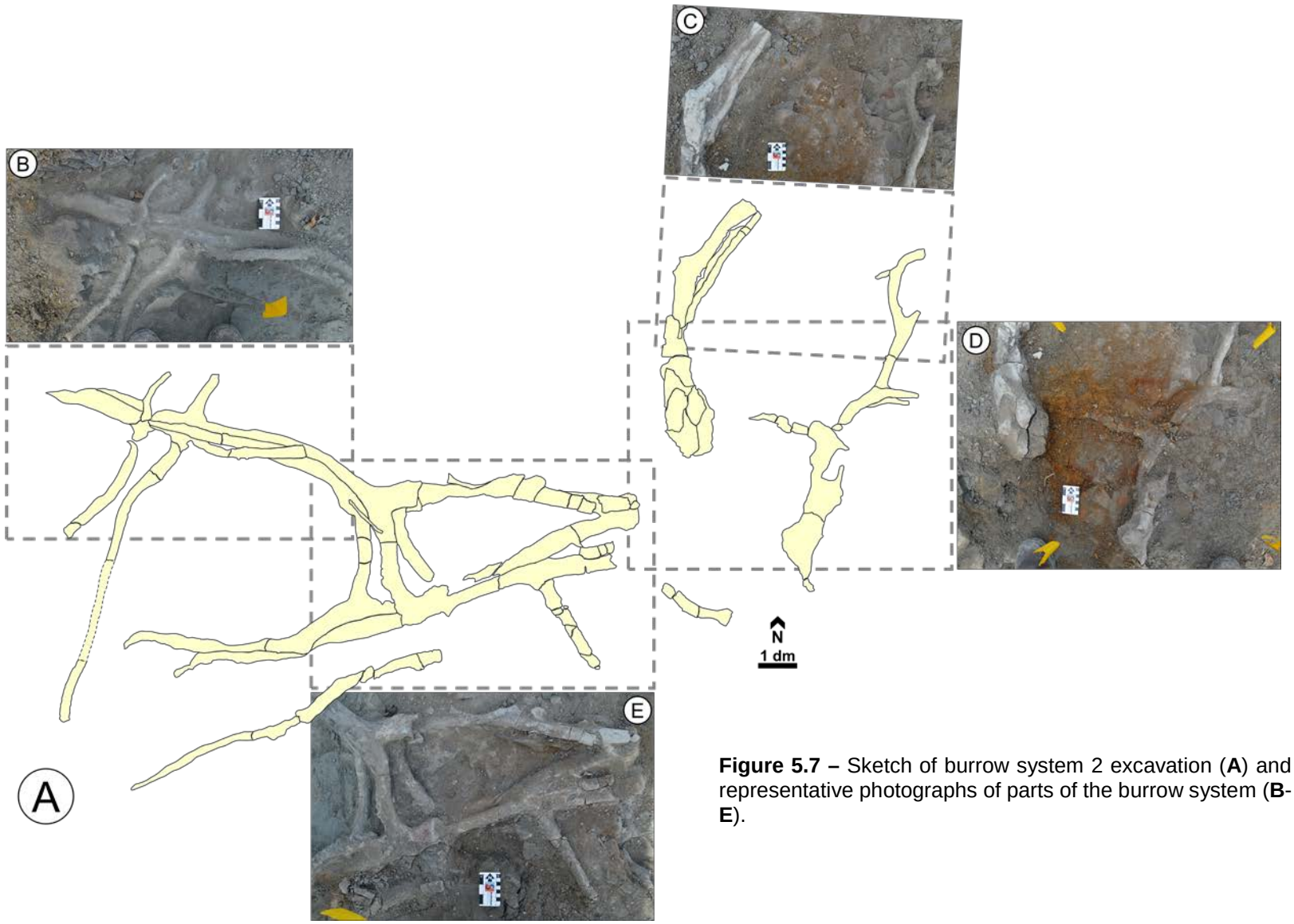

Figure 5.7 – Sketch of burrow system 2 excavation (**A**) and representative photographs of parts of the burrow system (**B**-**E**).

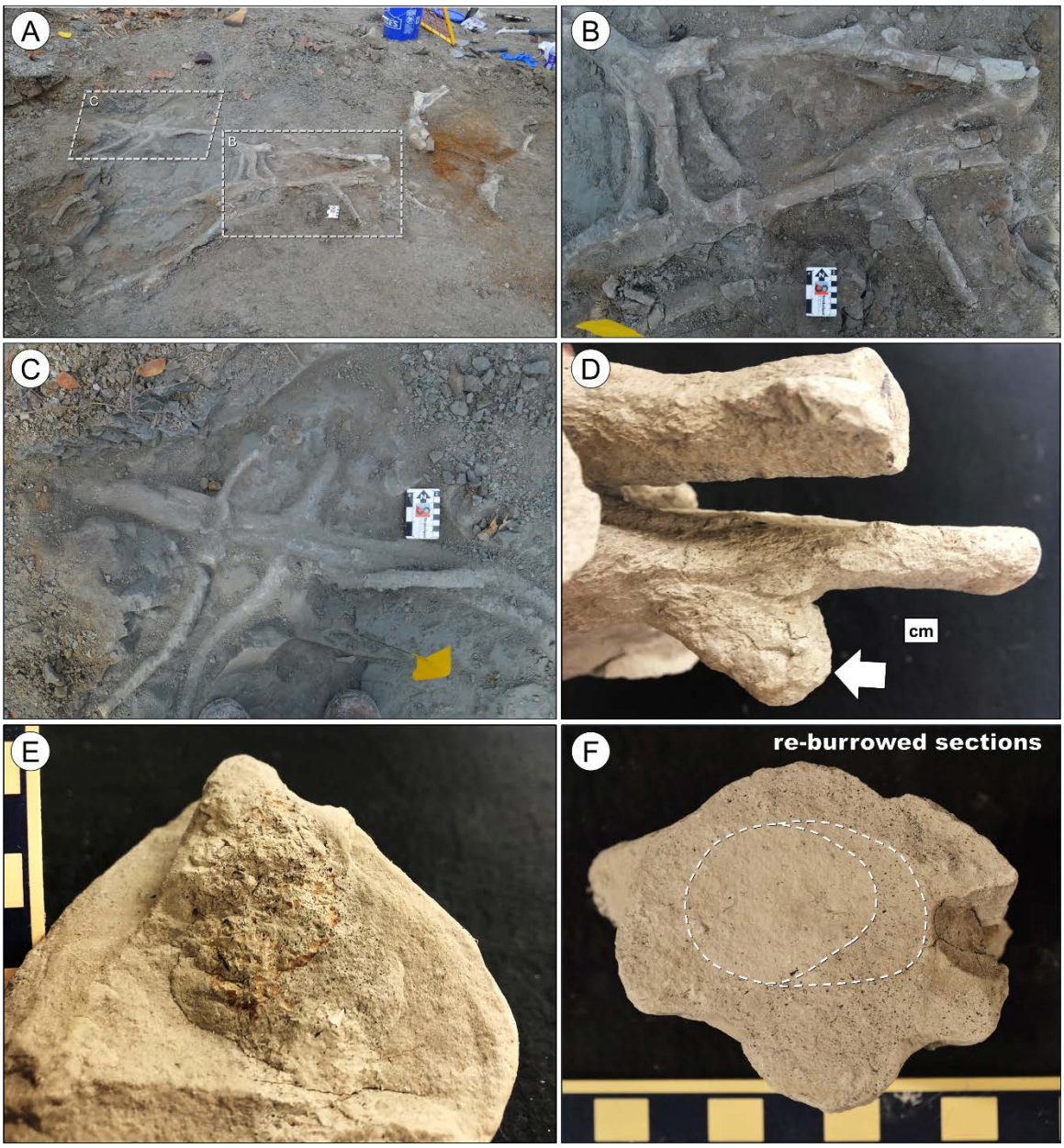

Figure 5.8 – Representative photographs of burrow system 2. **A**) Oblique photograph of entire excavated system. Dashed boxes show position of burrow segments depicted in B and C. **B**) Photograph of central part of system. **C**) Photograph of entwined burrow components. **D**) Photograph of bluntly terminating blind tunnel (arrow). **E**) Photograph of underside of blind tunnel with coarser fill containing concentrations of glauconite, fish debris(?), and possible organic matter. **F**) Transverse section of large burrow fill showing evidence of multiple phases of re-burrowing of burrow fill.

Figure 5.9 – Close-up photographs of bioglyphs on walls of burrows in system 2. **A**) Rhombohedral bioglyphs on the top of burrows. **B**) Close-up of rhombohedral bioglyphs. **C**) Transverse bioglyphs on the underside of a burrow.

5.3.4 Other Burrow Systems

While detailed study was limited to the excavated burrows systems, general observations also were made of other partially exposed burrow systems that were naturally weathering out from marls elsewhere along the exposure at Moscow Landing (Fig. 5.1B, 5.10A). Morphologies of these partial burrow systems are highly variable but commonly resemble parts of excavated burrow systems 1 and 2. Some are relatively simple, consisting of horizontal, branched burrows of relatively uniform width and with Y-shaped branch junctures (Fig. 5.10B). Others are more complex, consisting of parallel to subparallel, entwined segments of variable burrow width (Fig. 5.10C). One system is characterized by a horizontal, tightly meandering burrow segment that was apparently connected to a vertical shaft (Fig. 5.10D), features not documented in the excavated burrow systems. Burrow segments extracted from unit 18, like those in burrow system 2, are characterized by the wall bioglyphs and basal blind tunnels (Fig. 5.10E).

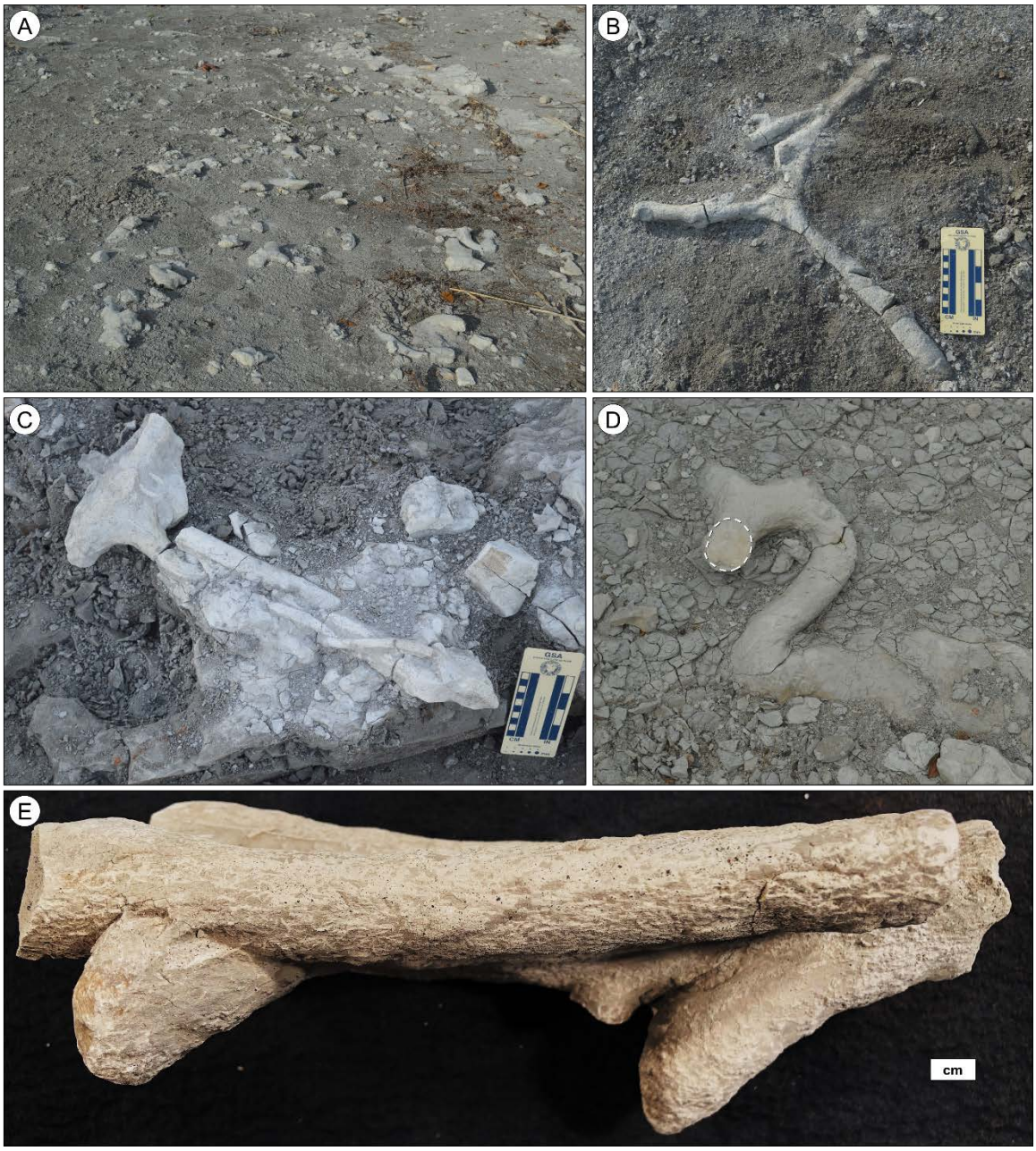

Fig. 5.10 – Select photographs of other burrow systems observed in Clayton marls. **A**) Burrow segments weathering out of Clayton marl in positive relief. **B**) Simple, Y-branched burrow segments. **C**) Entwined burrow segments. **D**) Tightly curved burrow segment. Dashed line indicates where horizontal burrow segment had connected to a vertical shaft. **E**) Burrow segment with rhombohedral bioglyphs and downwardly oriented, slightly acute blind tunnels.

5.4 Discussion

5.4.1 Ichnotaxonomic Affinities of Large Burrow Systems

Relatively large, branched burrows systems found in the stratigraphic record commonly have been assigned to one of four ichnogenera; *Ophiomorpha*, *Sinusichnus*, *Thalassinoides*, and *Spongeliomorpha*. The diagnostic features of these ichnogenera and common ichnospecies are summarized in Table 5.2 and are compared with those of the Clayton burrow systems below.

Structures assigned to *Ophiomorpha* are characterized by agglutinated pellet linings that reflect the trace makers efforts to stabilize their burrow walls in shifting, sand-dominated substrates deposited in physically unpredictable, relatively high-energy settings (Frey et al., 1978). The sharp, unlined walls of the Clayton burrow systems differ markedly from *Ophiomorpha*.

Branched burrow systems assigned to *Sinusichnus* are characterized by unlined, branched burrows that may exhibit elliptical cross sections and scratch-marked walls. However, the defining characteristic of *Sinusichnus* is the persistence of sinusoidal burrow segments that display more or less consistent amplitude/wavelength ratios (Belaústegui et al., 2014). A weakly sinusoidal segment is observed in burrow system 1 (Fig. 5.6B), and a tightly meandering segment is observed in one of the unexcavated, naturally exposed burrow systems (Fig. 5.10D). However, sinusoidal burrows are not pervasive in any of the observed Clayton burrow systems, hence assignment to *Sinusichnus* can be rejected.

Table 5.2 – Common large, branching ichnotaxa and their characteristics.

Ichnogenus	Diagnosis	Ichnospecies	Diagnosis
Ophiomorpha	Branched burrow systems featuring a distinct, agglutinated lining composed of pelletoids that are mammalated exteriorly and smoothed interiorly. Burrow fill may be structureless or consist of meniscate laminae. Rarely manifest as isolated shafts or tunnels, *Ophiomorpha* typically represent integrated burrow systems (Frey et al., 1978).	*O. nodosa*	Burrow lining consists of dense, regularly distributed discoid, ovoid, or irregular polygonal pellets (Frey et al., 1978).
		O. irregulaire	Burrow lining consists of sparse, irregularly distributed, ovoid to mastoid pellets (Frey et al., 1978).
		O. borneensis	Burrow lining consists of dense, regularly distributed bilobate pellets (Frey et al., 1978).
Thalassinoides	Single-plane to multi-planar branched burrow systems consisting of smooth-walled, unlined, cylindrical to elliptical components. Branches are Y- to T-shaped and typically enlarged at points of bifurcation (Frey and Howard, 1985).	*T. paradoxicus*	"Sparsely to densely but irregularly branched, subcylindrical to cylindrical burrows oriented at various angles with respect to bedding; T-shaped intersections are more common than Y-shaped bifurcations, and offshoots are not necessarily the same diameter as the parent trunk" (Howard and Frey, 1984).
		T. suevicus	"Predominantly horizontal, more or less regularly branched, essentially cylindrical components forming large burrow systems; dichotomous bifurcations more common than T-shaped branches" (Frey and Howard, 1985).
Spongeliomorpha	Single-plane to multi-planar branched burrow systems consisting of unlined, cylindrical to elliptical components ornamented with bioglyphs. Branches are Y- to T-shaped (Melchor et al., 2010).	*S. chevronensis*	"Ear-shaped" scratch pattern oblique to the main axis of the burrow (Melchor et al., 2010).
		S. sudolica	Rhombohedral scratch pattern and blind tunnels that terminate in blunt rounded ends (Gibert and Ekdale, 2010).
		S. carlsbergi	Transverse scratch pattern (Melchor et al., 2010).
		S. sicula	Longitudinal scratch pattern and vertically elongated, ovoid chambers (D'Alessandro and Bromley, 1995).
		S. iberica	Rhombohedral scratch pattern with blind tunnels that taper to an acute point (Gibert and Ekdale, 2010).
Sinusichnus	Horizontally developed, frequently branched burrow systems consisting of unlined, cylindrical to elliptical components. Segments commonly exhibit sinuosity. Burrow fill may consist of vertical spreiten (Gibert, 1996; Knaust et al., 2016).	*S. sinuosus*	Segments exhibit regular to irregular sinuosity. Branching is frequent, and spreiten are common (Gibert, 1996).
		S. seilacheri	Segments exhibit loose sinuosity and a locally bilobate floor containing faint, transverse to oblique striations (Knaust et al., 2016).
		S. priesti	Segments exhibit regular sinuosity, and burrow walls are ornamented with bioglyphs. Branching is frequent, and spreiten are common (Belaústegui et al., 2014).

Both *Thalassinoides* and *Spongeliomorpha* are described as single-plane to multi-planar, branched systems consisting of unlined, cylindrical to elliptical burrows with Y- to T-shaped branch junctions (Table 5.2). However, they are differentiated mainly based on the absence or presence of preserved bioglyphs on the burrow walls of *Thalassinoides* and *Spongeliomorpha*, respectively. The large burrow systems of the Clayton Formation are most closely allied with these two ichnogenera. Burrows with relatively smooth walls, e.g., those prevalent in burrow system 1, are assigned to *Thalassinoides*, whereas those burrows exhibiting extensive bioglyphs, e.g., those dominating burrow system 2 and other burrows in unit 18, are assigned to *Spongeliomorpha*.

Assignment of Clayton burrows to ichnospecies is more problematic. Two common ichnospecies of *Thalassinoides* are distinguished in post-Paleozoic deposits; *Thalassinoides paradoxicus* and *Thalassinoides suevicus* (Table 5.2). The *Thalassinoides* represented by burrow system 1 resembles *Th. suevicus* in that it is a large, predominantly horizontal burrow system wherein Y-shaped branches are more common than T-shaped branches. However, compared to *Th. suevicus*, branching in burrow system 1 is more irregular. Burrow system 1 resembles *Th. paradoxicus* with respect to irregular branching and intrasystem variability in burrow widths, but differs from this ichnospecies with regard to the lack of evident vertical or oblique burrow components, although such components had to have been present somewhere in the system. Weighing irregularity of branching and variable burrow diameters over burrow orientation, burrow system 1 is assigned here to *Thalassinoides paradoxicus*.

Five ichnospecies of *Spongeliomorpha* have been distinguished based primarily on (1) location and pattern of bioglyphs and (2) the presence/absence and character of blind tunnels or chambers that extend off main burrow segments (Table 5.2). The *Spongeliomorpha* identified in burrow system 2 is most closely allied with *Spongeliomorpha sudolica* and *Spongeliomorpha iberica*, based the prevalence of rhombohedral scratch patterns and presence of blind tunnels. Schlirf (2000) considered these two ichnospecies to be synonymous and suggested that *S. iberica* should be considered a junior synonym of *S. sudolica*, an approach provisionally accepted by Gibert and Robles (2005). However, Gibert and Ekdale (2010) later repudiated this argument and suggested that the following differences distinguish the two ichnospecies: (1) rhomboidal interspace between scratches is greater in *S. iberica*; (2) blind tunnels terminate in blunt, rounded ends in *S. sudolica* and taper to an acute point in *S. iberica*; and (3) the type material of *S. sudolica* features bioglyphs only on one side of the burrow, whereas *S. iberica* features bioglyphs on all sides of burrows. Following Gibert and Ekdale's (2010) argument, burrow system 2 is assigned to *Spongeliomorpha iberica*.

5.4.2 Paleoenvironmental Interpretation

The ichnofossils (C*hondrites*, *Planolites*) and burrow-mottled background ichnofabrics observed in the marls that host the large burrow systems — units 14 and 18 — are indicative of relatively soft substrates (i.e., softgrounds). In contrast, characteristics of the superimposed large burrow systems indicate that these host intervals were overconsolidated or firm when these structures were

emplaced. Evidence indicating that both *Thalassinoides paradoxicus* in unit 14 and *Spongeliomorpha iberica* in unit 18 were produced in firmgrounds include (1) sharp, unlined burrow walls, (2) limited compaction of burrow segments, (3) passive sediment infills derived from horizons lying 50-60 cm above the main burrow mazes, and (4) the apparent restriction of later-produced softground ichnofossils (e.g., *Chondrites*, *Planolites, etc.*) to these fills. In the case of *Spongeliomorpha* in unit 18 (e.g., burrow system 2), further evidence for firmground conditions is provided by scratch marks preserved on burrow walls. The presence of pervasive bioglyphs in burrow system 2 and their general absence in burrow system 1 suggest that the host marl of unit 18 was firmer or more consolidated than the host marl of unit 14. Nonetheless, both the *Thalassinoides* and *Spongeliomorpha* burrow systems in the Clayton Formation record firmground conditions and therefore can be assigned to the Glossifungites ichnofacies (Pemberton and Frey, 1985).

The development of firmgrounds and associated Glossifungites ichnofacies assemblages may be related to several processes. In relatively pure carbonate sequences, firmgrounds may develop as a result of winnowing or nondeposition and consequent incipient synsedimentary cementation at or near the seafloor (Bromley, 1975; Savrda, 2012). In more clastic-rich sequences, firmgrounds may develop in response to burial, dewatering, and subsequent erosional exhumation, by subaerial or submarine currents, of mud-rich sediments (Gingras et al., 2000). Firmgrounds developed in this manner can be linked to sea-level dynamics and commonly coincide, in a sequence stratigraphic

framework, with marine flooding surfaces; e.g., transgressive surfaces of erosion and other parasequence-bounding flooding surfaces (MacEachern et al., 1992). This appears to be the case for the Clayton firmground burrow systems.

In an earlier study of the Moscow Landing section, Savrda (1991) interpreted the limestone-marl couplets in the Clayton Formation (i.e., units 10-18) to be parasequences within a highstand system tract. In this context, the development of firmground *Thalassinoides paradoxicus* penetrating into unit 14 and other subjacent marls may record the culmination of shallowing-upward episodes that ultimately led to bottom-current winnowing and exhumation of partially consolidated marls. Savrda (1991) interpreted the unit 18-19 contact to be a co-planar sequence boundary-transgressive surface. This is supported by the high concentrations of glauconite and phosphate in unit 19 limestone. In this context, the development of firmground *Spongeliomorpha iberica* burrows preserved in unit 18 may be attributed to even deeper exhumation of consolidated marls caused by extended relative sea-level fall and consequent shoreface erosion. Deeper erosion of more thoroughly compacted marl at this sequence stratigraphic surface is consistent with the well-developed bioglyphs on *Spongeliomorpha iberica* in unit 18.

Firmgrounds developed in the manner described above intrinsically involve depositional hiatuses during which substrates may be available for colonization for an extended period of time. Hence, the excavated burrow systems may represent *cumulative* structures that record the integrated work of multiple organisms, including adult and juvenile forms of the same species and/or

multiple species of burrowing organisms. The cumulative nature of these structures complicates interpretations of trace makers and their behaviors.

5.4.3 Potential Tracemakers

One inherent difficulty in ichnology is the identification of specific trace makers. This is because body fossils are very rarely preserved in direct association with their corresponding biogenic structures, and different organisms with similar body plans and behaviors can produce morphologically similar structures (Buatois and Mángano, 2011). Commonly, only the general taxonomic affinities of trace makers can be inferred. Such inferences are based morphological comparisons with (1) rare ichnofossils that are associated with body fossils of likely trace makers and (2) architectures of modern biogenic structures for which producers are known. Based on such comparisons, *Thalassinoides* and *Spongeliomorpha* (and the other ichnotaxa summarized in Table 5.2) are normally attributed to marine decapod crustaceans, which possess rigid appendages that facilitate burrowing in soft to firm substrates and commonly generate and inhabit variably branched, open burrow systems (Ekdale and Bromley, 2003). Such decapod crustaceans are diverse and include shrimps (e.g., thalassinideans), crabs (brachyurans), and lobsters (astacideans). Aspects of the Clayton burrow systems compare favorably with modern and ancient biogenic structures attributed to these three groups.

The architectures of modern shrimp burrows have been documented in numerous studies that employ resin-casting techniques (e.g., Braithwaite and Talbot, 1972; Griffis and Suchanek, 1991; Nickell and Atkinson, 1995; Tamaki

and Ueno, 1998; Kinoshita, 2002; Pervesler and Hohenegger, 2006). A major conclusion that can be drawn from these studies is that burrow morphologies are extremely variable, reflecting either intraspecific behavioral plasticity (e.g., Miller and Curran, 2001) or differences in feeding strategies and construction protocols among shrimp species (e.g., Griffis and Suchanek, 1991). Features commonly observed in modern shrimp burrow systems include the presence of a wide inhalant shaft and a narrow, smooth, undulating exhalant shaft; a sediment mound at exhalant shaft openings; downward directed, central, blind-ending shafts; and horizontally-developed planes of tunnels and chambers (Griffis and Suchanek, 1991). Most of these features were not encountered during the excavation of the Clayton burrow systems due to nonpreservation and/or sparse distribution of vertical components. However, deeper horizontal components of some modern shrimp burrow systems (e.g., the “deep reticulate” forms of Griffis and Suchanek, 1991) bear some resemblance to those in burrow systems 1 and 2. Hence, it is plausible that one or more species of shrimp constructed the *Thalassinoides* and *Spongeliomorpha* observed in the Clayton Formation.

Modern crab burrows also have been studied using resin-casting techniques (e.g., Hayasaka, 1935; Braithwaite and Talbot, 1972; Hill and Hunter, 1973; Allen and Curran, 1974). In general, crab burrows in supra- and intertidal settings exhibit simple curves and feature limited branching or lack branches altogether (Braithwaite and Talbot, 1972). However, burrow casts retrieved in settings influenced by normal marine salinities or in subtidal settings may be more complex and exhibit a higher degree of branching and lateral

interconnectivity at depth (Chapman and Rice, 1971; Allen and Curran, 1974). The excavated Clayton burrow systems at least crudely resemble the deeper elements of modern subtidal crab burrows.

In their study of Cretaceous strata of Portugal, Carvalho et al. (2007) described *Thalassinoides* burrow systems closely associated with exceptionally preserved exoskeletons of the fossil lobster *Mecochirus rapax*, the presumed trace maker. The burrows they describe resemble the Clayton burrow systems in that they are predominantly horizontal, feature Y-shaped bifurcations, exhibit enlarged burrow diameters at bifurcation sites, and are elliptical in cross section. The lobster-associated burrows described by Carvalho et al. (2007) are considerably larger than the Clayton structures; burrow widths and lengths can exceed 11 cm and 1 m, respectively. Nonetheless, it is possible that smaller lobsters contributed to the construction of Clayton burrow systems.

In summary, the Clayton burrow systems were most likely produced by decapod crustaceans, although the specific group(s) of crustaceans cannot be inferred with confidence. Given their cumulative nature, these firmground burrow systems may have been produced by multiple individuals and species operating contemporaneously or during different phases of associated depositional hiatuses.

5.4.4 Behavioral Implications

Decapod crustaceans construct burrows for various reasons, depending on their mode of feeding. Some burrow systems are primarily dwellings produced by suspension feeders or surface detritus feeders, whereas others may be

constructed in the process of active deposit feeding or gardening (D'Alessandro and Bromley, 1995; Gibert and Robles, 2005; Gibert and Ekdale, 2010).

Given their production in firmgrounds, the large burrows systems in the Clayton Formation likely were constructed as semi-permanent to permanent dwelling structures. However, how the trace makers obtained nutrition is not clear. Burrow systems of suspension feeders normally require multiple vertical shafts to facilitate adequate water circulation (Gibert and Ekdale, 2010). Given the areal extent of the Clayton burrow systems and the paucity of vertical burrow components therein, production by suspension feeders seems unlikely. However, as demonstrated by Nickell and Atkinson (1995), some modern suspension-feeding shrimp may construct as few as two shafts (an exhalant shaft and an inhalant shaft) in a single complex system. Hence, suspension feeding cannot be excluded altogether.

The crustaceans responsible for the large Clayton burrows likely were not deposit feeders. The firmground substrates into which they burrowed would have contained little to no labile organic detritus on which to feed. However, organic food sources may have been available at the seafloor and, hence, the trace makers may have been surface detritus feeders. Alternatively, the trace makers may have been gardeners. Some crustaceans (e.g., thalassinidean shrimp) are known to collect and store plant material in their burrows, and, after maturation, this organic material is later consumed by the trace makers (Griffis and Suchanek, 1991). Gibert and Ekdale (2010) have suggested that common blind tunnels observed in some *Spongeliomorpha* ichnospecies may represent alcoves

created for the storage and maturation of organic detritus. The blind tunnels in *Spongeliomorpha iberica* in unit 18 could be interpreted in a similar manner. However, there is no preserved evidence to indicate that these features once served as repositories for organic detritus.

In summary, the behaviors of the trace makers that constructed the large burrow systems in the Clayton Formation cannot be confidently established. Although deposit feeding can be excluded, the trace makers may have been suspension feeders, detritus feeders, gardeners, or some combination thereof.

5.5 Summary

Large, highly irregular, branching burrow systems hosted in unit 14 and unit 18 marls of the Clayton Formation exposed at Moscow Landing are assigned to *Thalassinoides paradoxicus* and *Spongeliomorpha iberica*, respectively. While background ichnofabrics of the host marls are indicative of softground conditions, characteristics of the large burrow systems indicate that host intervals were firm when these structures were emplaced. Hence, both *Thalassinoides* and *Spongeliomorpha* burrow systems are assigned to the Glossifungites ichnofacies. Firmground conditions at each of these horizons developed in response to erosional exhumation of semiconsolidated marls at marine flooding surfaces, which is consistent with previous sequence stratigraphic interpretations (Savrda, 1991).

Based on morphological comparisons with fossils and modern biogenic structures for which producers are known, the trace makers of the Clayton burrow systems are inferred to be decapod crustaceans. Given their cumulative

nature, the burrow systems may have been produced by multiple individuals and species operating contemporaneously. The trace makers likely were not deposit feeders but instead may have constructed the burrows for the purpose of suspension feeding, detritus feeding, gardening, or some combination thereof.

6. Clayton Chalk

6.1 Introduction

During the Cretaceous, high sea-level stands and ocean chemistry resulted in deposition of shelf-sea chalks worldwide (Ekdale and Bromley, 1984; Savrda, 2012), including the chalks of the Cretaceous Selma Group, eastern Gulf coastal plain (e.g., Mooreville, Demopolis, and Prairie Bluff chalks in western Alabama and eastern Mississippi; Fig. 6.1). Owing to overall regression, draining of epeiric seas, and increased flux of clastic sediments to continental margins at the end of the Mesozoic, deposition of carbonate oozes during the Paleogene and Neogene generally has been restricted to deeper, more distal depositional settings. The chalk bed (bed 23) exposed at Moscow Landing (Fig. 6.2), hereafter referred to as the Clayton chalk, represents a rare exception, recording a brief early Paleocene (Danian) episode of carbonate ooze deposition in the Gulf coast region. As noted earlier, the objectives of this chapter are to characterize the ichnosedimentology of the Clayton chalk, compare the Clayton chalk with chalk-dominated units of the Selma Group, interpret depositional conditions for the Clayton chalk, and outline implications for early Paleocene sea-level dynamics.

6.2 Field Description of the Clayton Chalk

The Clayton chalk is a light gray to white, moderately indurated chalk exposed continuously at the Moscow Landing section (Fig. 6.3) where it forms a

subtle ledge between relatively thick (0.75-2.25 m), dark olive gray, poorly indurated marls. Thickness of the chalk is generally constant at ~25 cm with one exception; at one location, the chalk was nearly completely truncated by a broad (8-10 m), shallow (~20 cm) scour surface mantled by a bivalve shell lag (Fig. 6.4).

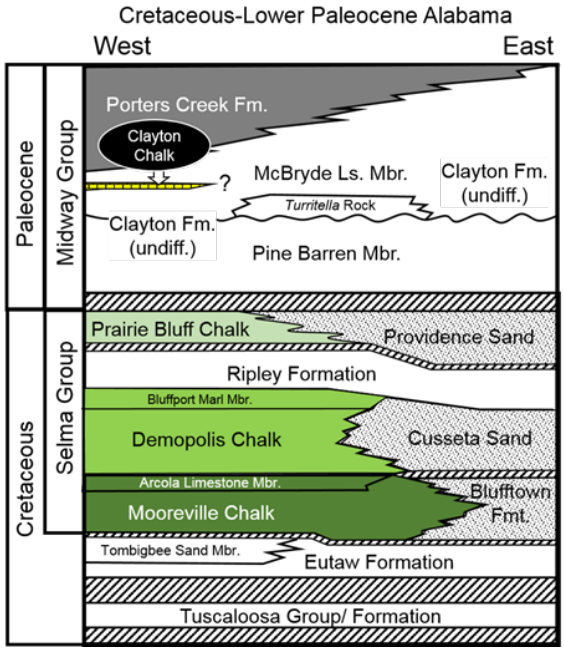

Figure 6.1 – Distribution of Cretaceous and Lower Paleocene strata in Alabama coastal plain. Cretaceous and Paleocene chalks are highlighted in greens and yellow, respectively.

6.3 Sedimentology of the Clayton Chalk

The Clayton chalk is the purest carbonate unit in the Clayton Formation. $CaCO_3$ contents of the Clayton chalk range from 79.37% to 83.74% ($\bar{x}$ = 81.81%, n=4). In contrast, $CaCO_3$ contents in the immediately subjacent marl range from 47.57% to 62.95 % ($\bar{x}$ =53.34 %, n=3) (Table 6.1; Fig. 6.5).

As viewed in thin section, the Clayton chalk proper can be classified as a slightly phosphatic foraminiferal wackestone (Fig. 6.6A-D). Skeletal allochems, which float in a fine micritic matrix, are dominated by planktonic and benthic foraminifera (Fig. 6.6B). Subordinate silt or sand-sized components include

bivalve and echinoderm fragments, bone fragments, and rare identified phosphatic grains (Fig. 6.6C, D). The chalk includes virtually no recognizable silt- or sand-sized clastic grains.

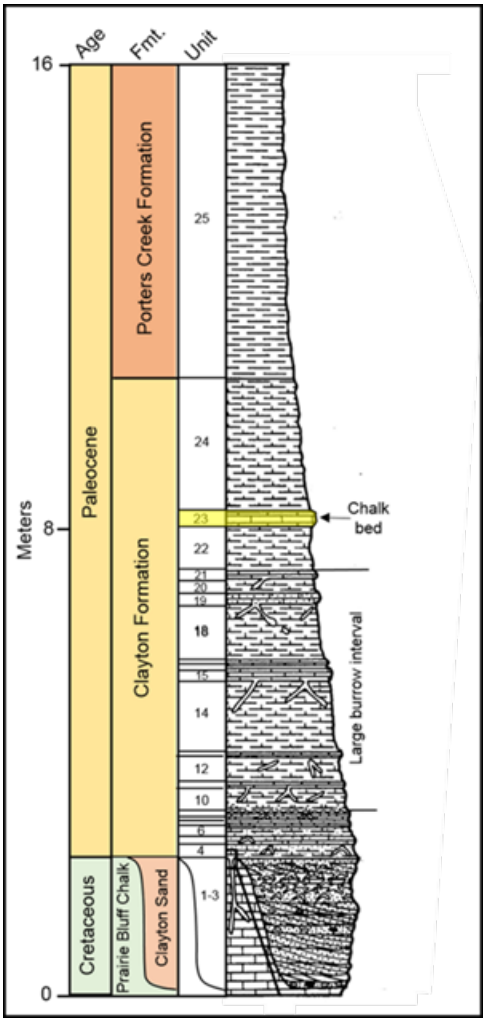

Figure 6.2 – Stratigraphic column depicting position of the Clayton chalk (highlighted in yellow) in the Moscow Landing section (modified from Savrda, 1991).

As viewed in thin section, the marl underlying the Clayton chalk similarly can be classified as a slightly phosphatic foraminiferal wackestone (Fig. 6.6E, F). However, compared to the chalk, foraminifera are less abundant, and the silt- or sand-sized fraction includes rare quartz (<1%) as well as phosphatic grains (Fig. 6.6E).

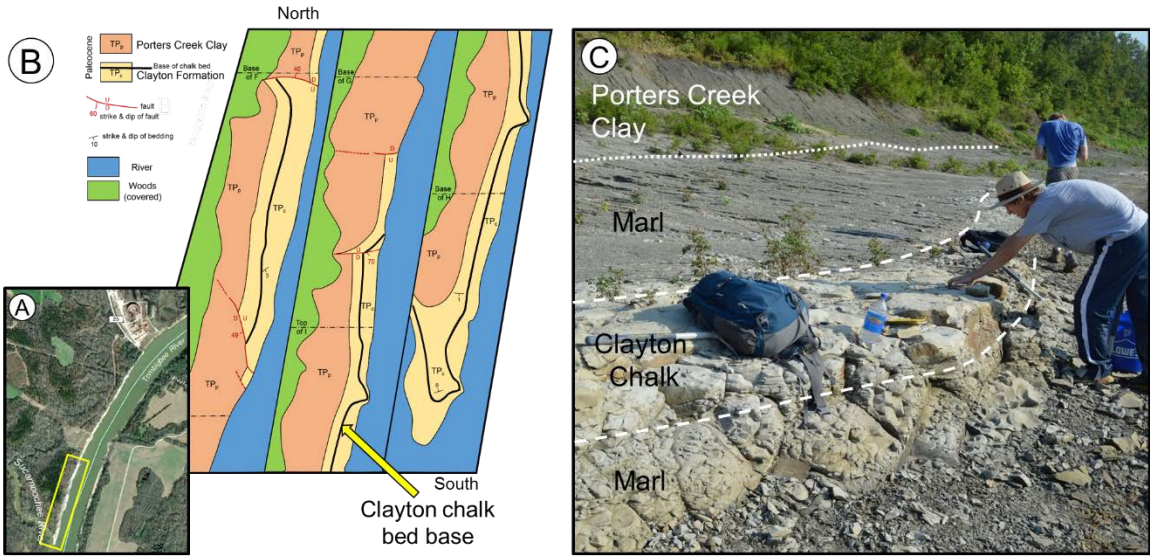

Figure 6.3 – Exposure of Clayton chalk at the Moscow Landing section. **A)** Southern end of Moscow Landing section where the Clayton chalk is best exposed. **B**) Strip map of section of Moscow Landing exposure highlighted in A. **C**) Natural exposure of Clayton chalk and surrounding strata.

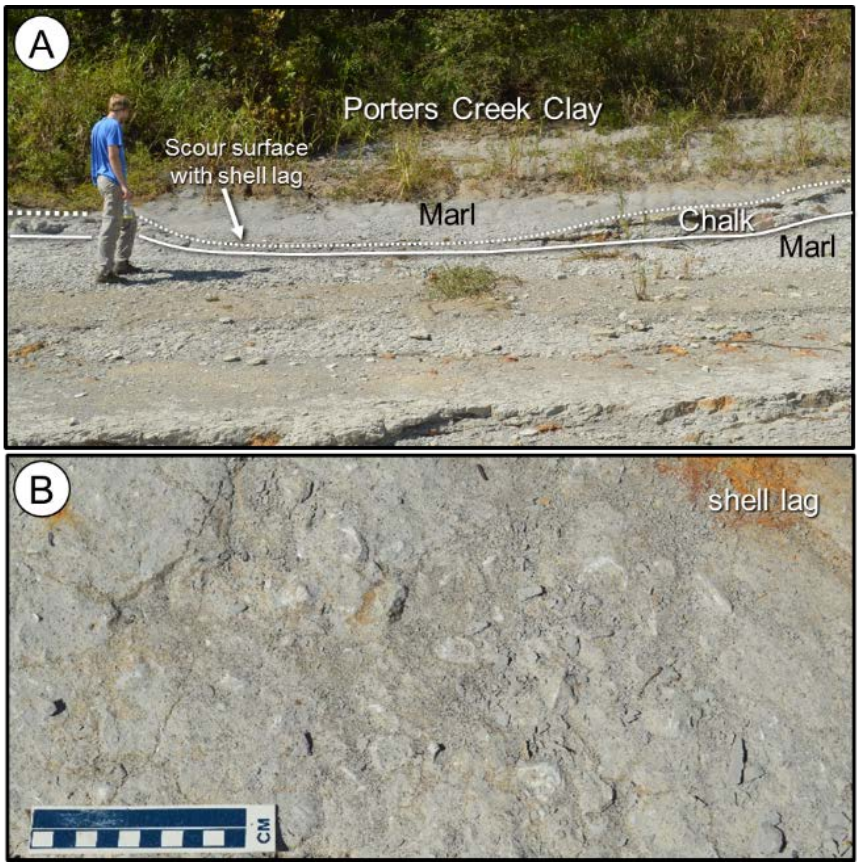

Figure 6.4 – Broad, shallow scour surface in Clayton chalk. **A**) Profile view of scour surface. **B**) Close-up photograph of shell lag mantling the scour surface.

Table 6.1 – Carbonate contents of Clayton chalk (unit 23) and subjacent marl (unit 22) based on weight loss after acid digestion in HCl (see Fig. 6.5).

Sample	$CaCO_3$ %	Average %
CK-8: unit 23 (chalk)	81.69	81.81
CK-7: unit 23 (chalk)	82.44	
CK-6: unit 23 (chalk)	83.74	
CK-5: unit 23 (chalk)	81.79	
CK-4: unit 23 (chalk)	79.37	
CK-3: unit 22 (marl)	62.95	53.34
CK-2: unit 22 (marl)	49.51	
CK-1: unit 22 (marl)	47.57	

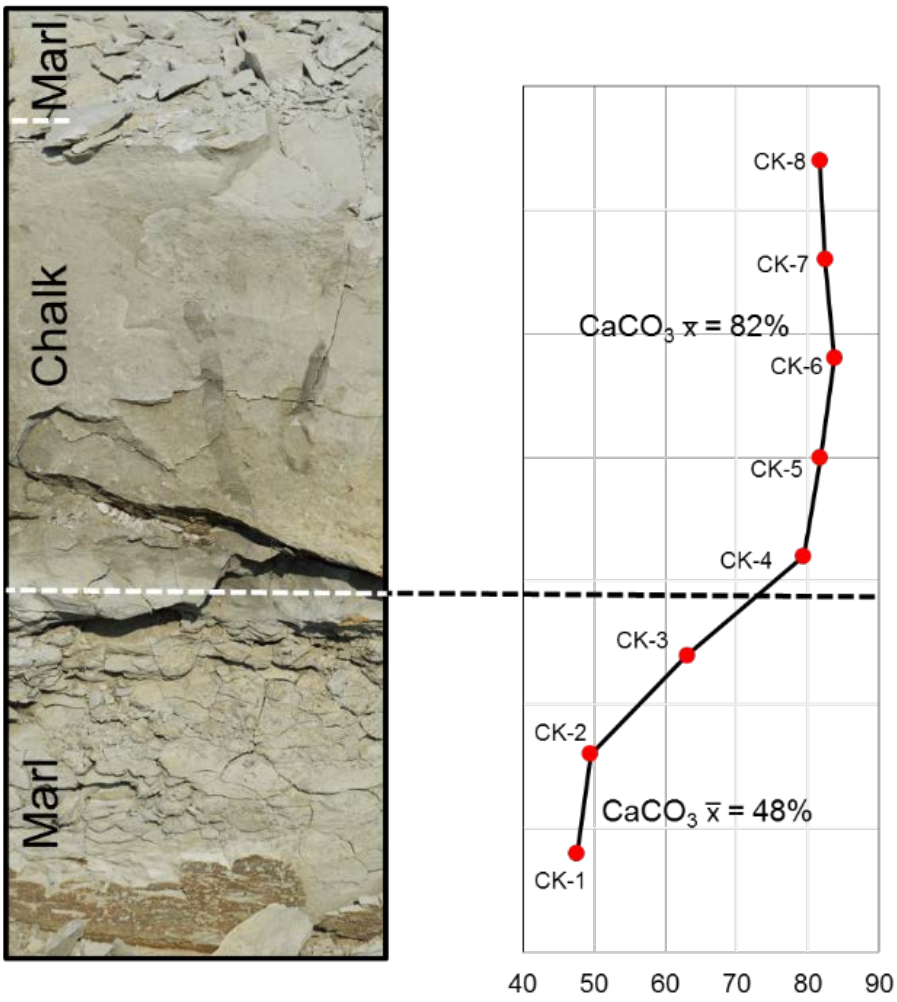

Figure 6.5 – Depiction of $CaCO_3$ contents in Clayton chalk and subjacent marl.

6.4 Ichnology of the Clayton Chalk

6.4.1 Field Expression

Both the Clayton chalk and underlying marl are completely bioturbated. However, the natural field expression of ichnofabrics in the Clayton chalk and subjacent marl is generally poor (Fig. 6.7A). On typical, highly weathered surfaces, ichnofossils are generally indistinct. Exceptions include the localized expression on bedding-parallel surfaces of relatively large, branched *Thalassinoides* burrows, the fills of which are typically cross cut by *Chondrites* (Fig. 6.7B), and rare occurrences of *Teredolites* (shipworm borings) associated with poorly preserved, lignitized wood clasts (Fig. 6.7C). Ichnofabric expression is slightly improved on fresh fracture surfaces (Fig. 6.7D). However, detailed ichnofabric analyses required the observation of vertical rock surfaces prepared from sample blocks in the laboratory.

6.4.2 Ichnofabric Expression on Prepared Rock Slabs

General Ichnofabric Expression

Ichnofabric expression on smoothed vertical surfaces is generally very good, owing in part to color contrast between distinct trace fossils and host sediments. The Clayton chalk bed proper is characterized by darker-colored ichnofossils superimposed upon a lighter homogenous background fabric; distinct burrows were emplaced during and shortly after chalk deposition and define what Savrda (2014) referred to as a dark-on-light (DOL) piped zone. The upper ~30 cm of the subjacent marl is characterized by lighter-colored ichnofossils overprinted on a darker homogeneous background; distinct

ichnofossils here were emplaced during chalk deposition and define a light-on-dark (LOD) piped zone (Fig. 6.8). To best evaluate conditions associated with chalk deposition, ichnologic observations focused on the Clayton chalk proper and subjacent LOD piped zone. Notably, both of these horizons are characterized by the same assemblage of distinct ichnofossils.

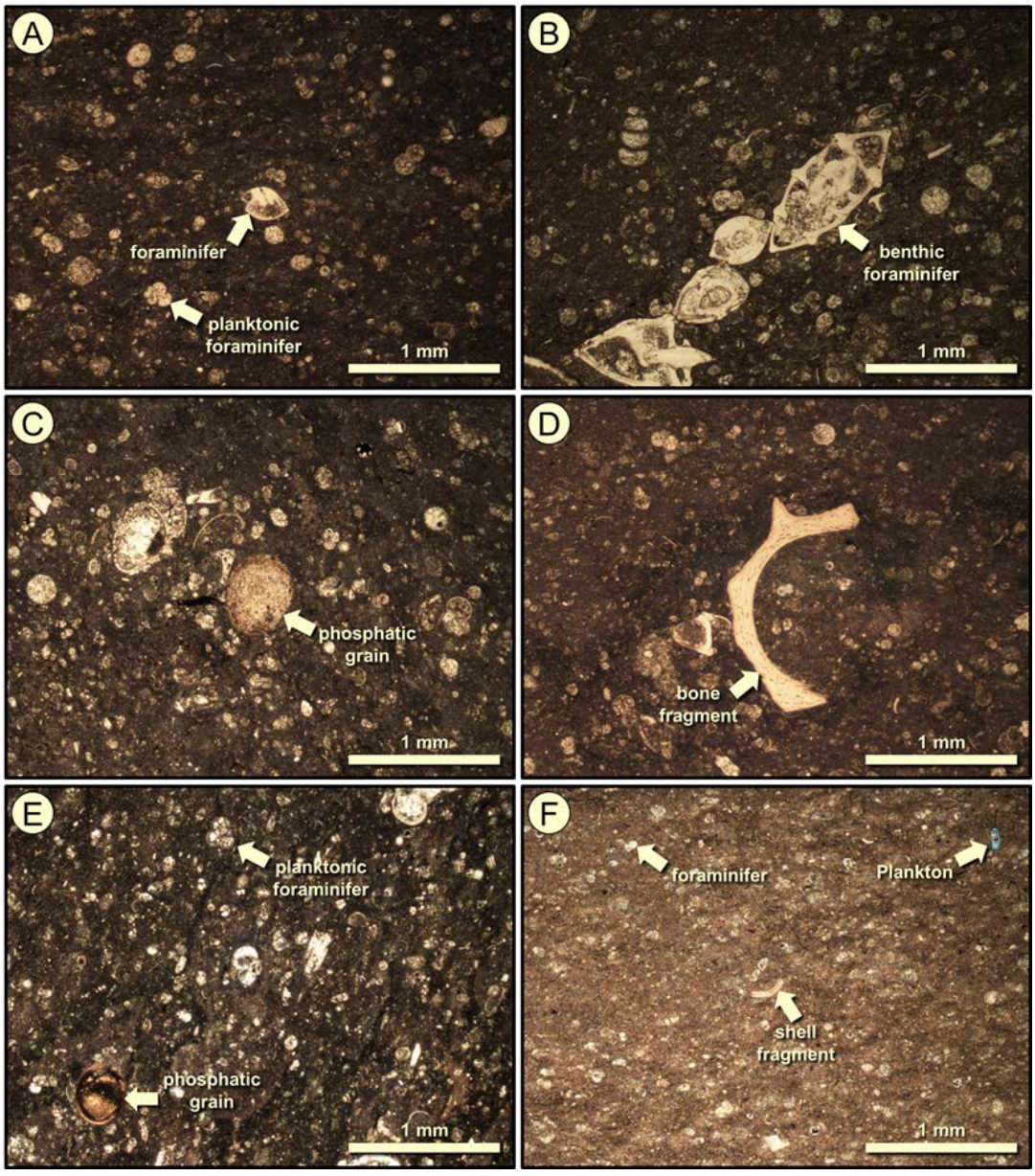

Figure 6.6 – Photomicrographs of Clayton chalk (**A** – **D**) and underlying marl (**E**, **F**). **A, B**) Planktonic and benthic foraminifera surrounded by dark micritic matrix. **C, D**) Phosphatic grains (bone fragments). **E, F**) Foraminifera, phosphatic grains, and unidentified shell fragments.

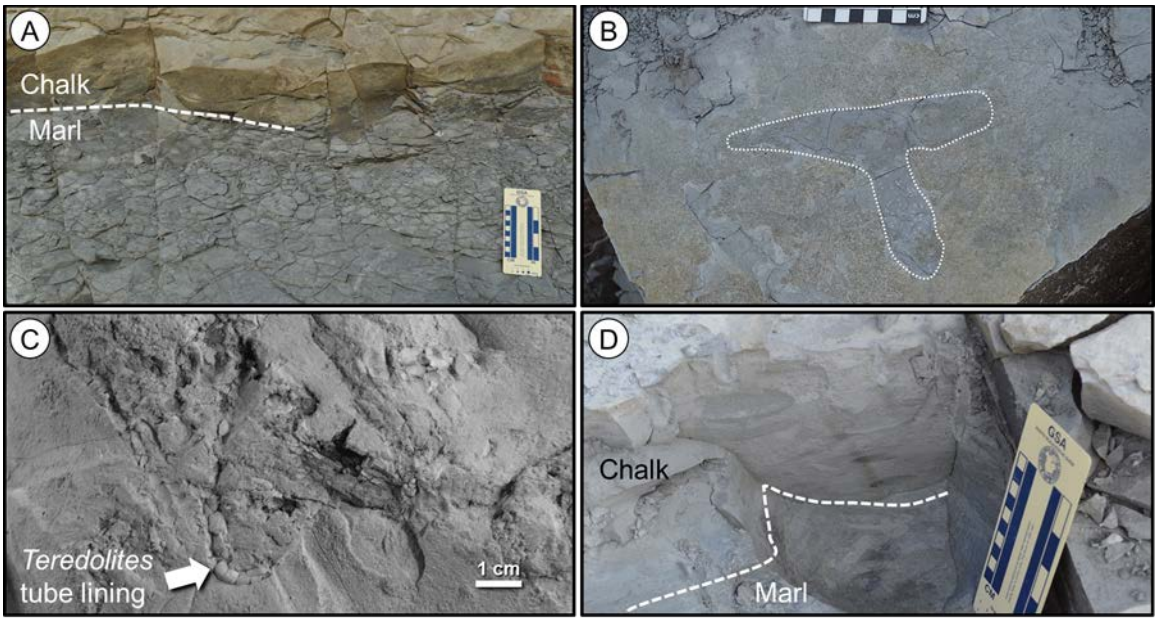

Figure 6.7 – Field expression of ichnofabrics of Clayton chalk and underlying marl. **A**) Weathered surface of Clayton chalk and underlying marl. **B**) Ill-defined *Thalassinoides* with fill reburrowed with *Chondrites*. **C**) *Teredolites* tube linings (arrow) associated with lignitized wood. **D**) Fresh subvertical fracture surface of Clayton chalk and underlying marl.

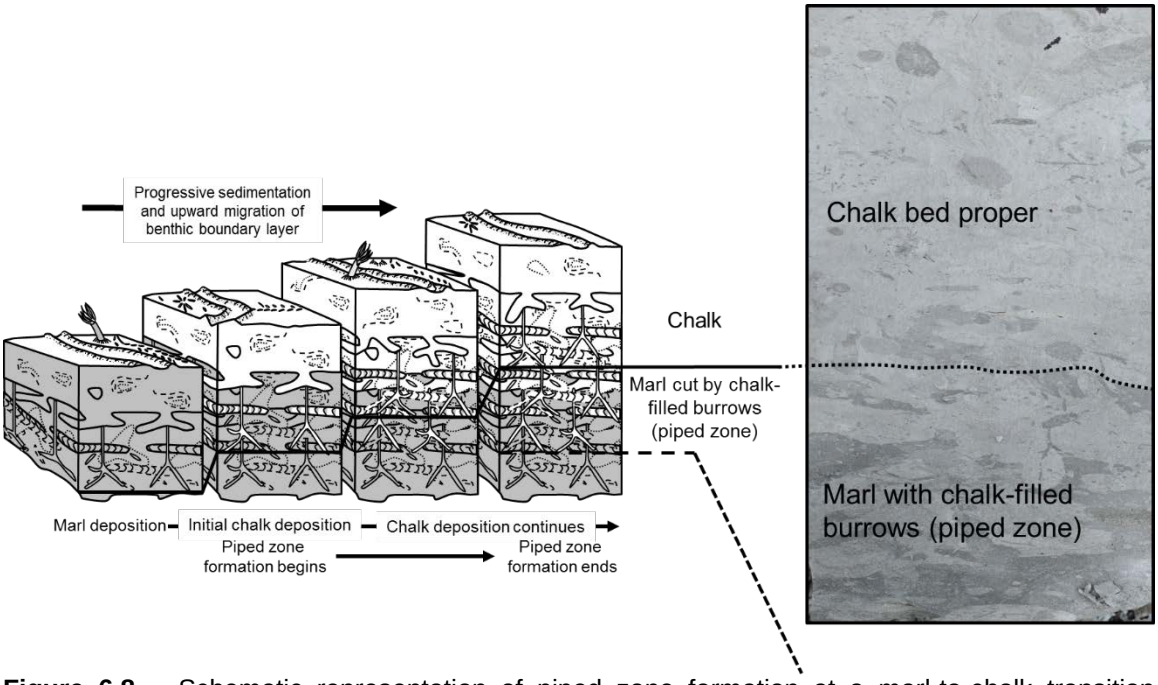

Figure 6.8 – Schematic representation of piped zone formation at a marl-to-chalk transition (modified from Savrda, 2014).

Recurring Ichnotaxa

Both the Clayton chalk and subjacent piped zone contain a moderately diverse ichnofossil assemblage that includes abundant *Chondrites*, common *Thalassinoides*, *Planolites*, *Zoophycos*, and *Teichichnus*, and rare *Taenidium*, *Palaeophycus*, and *Phycosiphon*. This assemblage exemplifies the Zoophycos ichnofacies (Savrda, 2012). Examples of these ichnotaxa are illustrated in figures 6.9 and 6.10.

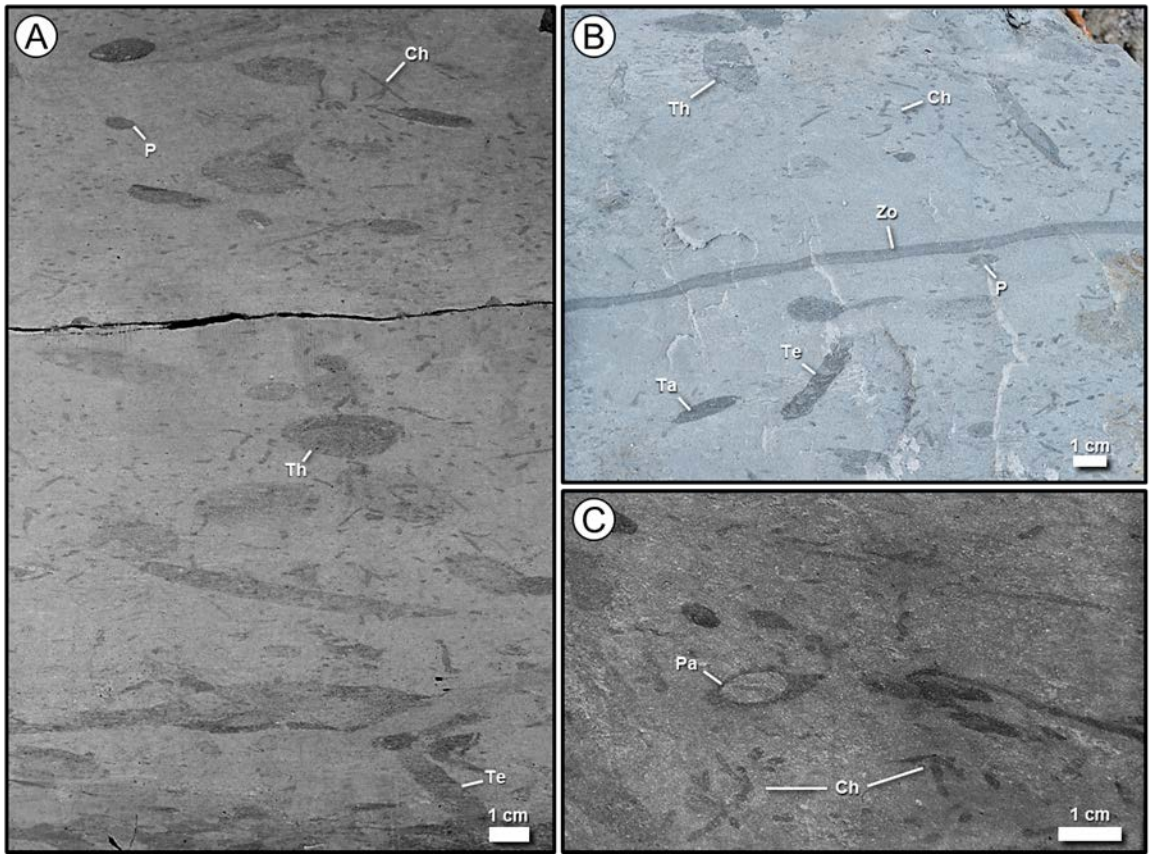

Figure 6.9 – Representative ichnofabrics and ichnofossils in the Clayton chalk proper. Th = *Thalassinoides*, Ch = *Chondrites*, Zo = *Zoophycos*, P = *Planolites*, Te = *Teichichnus*, Ta = *Taenidium,* and Pa = *Palaeophycus*.

Chondrites is the most common ichnotaxa observed. These branching burrow systems are typically manifest on vertical surfaces as isolated horizontal

to vertical, short to elongate blebs, although slab surfaces locally intersect branch junctions (Figs. 6.9, 6.10). Burrow diameters range from 0.75 mm to 1.5 mm ($\bar{x}$ = 1 mm, n = 13). *Chondrites* generally cross cuts all other ichnofossils and occurs at the deepest levels of the piped zone, indicating that the tracemaker (an unknown worm-like organism) occupied the deepest substrate tier.

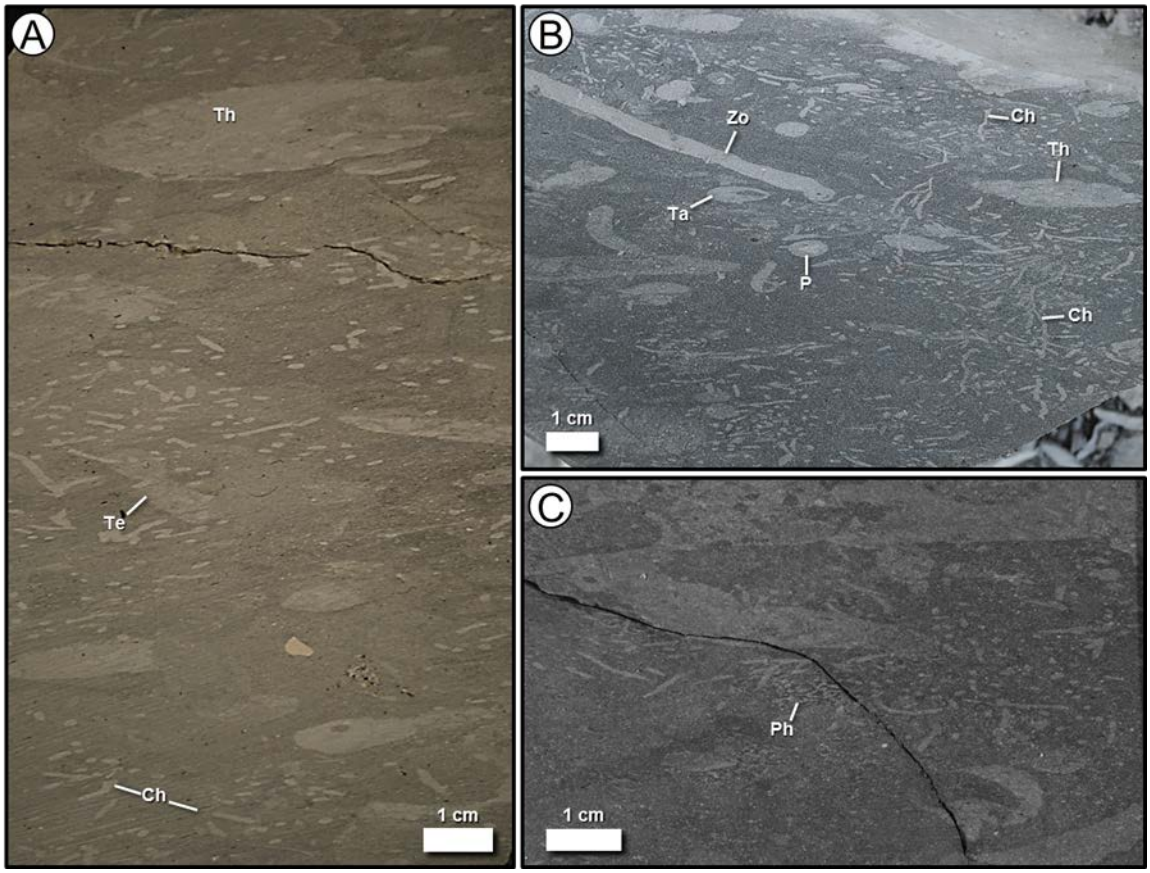

Figure 6.10 – Representative ichnofabrics and ichnofossils in piped zone beneath the Clayton chalk. Th = *Thalassinoides*, Ch = *Chondrites*, Zo = *Zoophycos*, P = *Planolites*, Te = *Teichichnus*, Ta = *Taenidium,* Ph = *Phycosiphon*.

Structures referred to as *Thalassinoides* are generally manifest on vertical slab surfaces as relatively large, circular to ovate masses; branch junctures were rarely intersected by two-dimensional slab surfaces (Fig. 6.9A, B; Fig. 6.10A, B) . Burrow diameters range from 7 mm to 26 mm ($\bar{x}$ = 11.25 mm, n = 8). *Thalassinoides* is commonly cross cut by *Chondrites* and other traces, indicating

that the tracemakers—crustaceans of some type—occupied a relatively shallow substrate tier.

Traces assigned to *Planolites* are manifest as moderately sized, circular to ovate masses (Fig. 6.9A, B; Fig. 6.10B). Burrow diameters range from 2 mm to 10 mm ($\overline{x}$ = 5.06 mm, n = 16). Owing to morphological similarities as viewed in two-dimensional vertical plans, *Planolites* and smaller-diameter *Thalassinoides* were not always readily distinguishable on prepared block-sample surfaces.

Although also observed in the chalk bed proper (Fig. 6.9B), *Zoophycos* is more common in the underlying piped zone (i.e., in the subjacent marl; Fig. 6.10B). Traces assigned to this ichnogenus are manifest as horizontal to sub-horizontal, elongate structures which represent cross-sectional views of subhorizontal planar spreiten. Laminae are visible locally. Spreite heights range from 3.5 mm to 5 mm ($\overline{x}$ = 4.25 mm, n = 6). *Zoophycos* is commonly cross cut by *Chondrites* and locally cross cuts *Thalassinoides*, indicating that the tracemakers—possibly worms of some type (Bromley, 1991)—occupied an intermediate substrate tier.

Traces assigned to *Teichichnus* (Fig. 6.9A; Fig. 6.10A) are manifest as vertical to sub-vertical structures, some with a marked zigzag pattern. Laminae are generally poorly expressed. Spreite widths range from 2.5 mm to 5 mm ($\overline{x}$ = 4.125 mm, n = 4). *Teichichnus* is commonly cross cut by *Chondrites* and locally cross cut by *Planolites*, indicating that the tracemakers, likely worm-like organisms, may have occupied a shallow to intermediate substrate tier.

Taenidium is manifest on vertical slab surfaces as circular, ovate, or elongate masses (Fig. 6.9B; Fig. 6.10B) that appear to feature a meniscate backfill. Burrow diameters range from 2.5 mm to 5 mm ($\overline{x}$ = 3.7 mm, n = 5). Rarity of cross-cutting relationships among *Taenidium* and other traces precludes inferences regarding relative substrate tier depth.

Palaeophycus is similarly manifest on vertical slab surfaces as circular to ovate masses. This trace is distinguished from *Taenidium* based on the absence of meniscate backfill and from *Planolites* based on the presence a thin lining (Fig. 6.9C). Burrow diameters range from 7 to 13 ($\overline{x}$ = 8.25 mm, n = 4). Rarity of cross-cutting relationships among *Palaeophycus* and other traces precludes inferences regarding relative substrate tier depth.

Phycosiphon appears to be limited to the piped zone where they are difficult to distinguish due their small size and limited contrast with host sediments. These are manifest as clusters small-scale structures consisting of darker burrow cores surrounded by lighter mantles (Fig. 6.10C). Diameters of burrow cores range from 0.1 to 0.5 ($\overline{x}$ = 0.28 mm, n = 3).

6.5 Discussion

6.5.1 Ichno-sedimentologic Comparison with Selma Chalks

General sedimentologic and ichnologic characteristics of the Clayton chalk are compared with those of chalk-dominated units of the Cretaceous Selma Group (i.e., Mooreville, Demopolis, and Prairie Bluff Chalks; Fig. 6.1) in Table 6.2. Other calcareous members of the Selma Group (e.g., the calcispheric Arcola Limestone member of the Mooreville Chalk and Blufftown Marl Member of the

Demopolis Chalk were excluded). As described below, the Clayton chalk compares most favorably with the Demopolis Chalk.

Table 6.2 – Ichno-sedimentologic comparisons among the Clayton chalk and the Cretaceous Prairie Bluff Chalk, Demopolis Chalk, and Mooreville Chalk.

Unit	Sediment Character	Recurring Ichnotaxa										Sources
		Chondrites	Cylindrichnus	Palaeophycus	Phycosiphon	Planolites	Rosselia	Skolithos	Taenidium	Teichichnus	Thalassinoides	Zoophycos	
Clayton chalk	Chalk $CaCO_3$ – 82%												This study
Prairie Bluff Chalk	Sandy, glauconitic chalk $CaCO_3$ – 72%												Frey and Bromley, 1985
Demopolis Chalk	Chalk $CaCO_3$ – 80%												Frey and Bromley, 1985; Locklair and Savrda, 1998a
Mooreville Chalk	Clayey-chalk $CaCO_3$ – <75% Szabo and Beg (1977)												Frey and Bromley, 1985

The unnamed lower member of the Mooreville Chalk is a clayey chalk or a very chalky clay with a relatively low average $CaCO_3$ content of less than 75% (Szabo and Beg, 1977). This unit is sparsely fossiliferous, indistinctly burrow mottled, glauconitic, and fissile locally; it is consistently rich in terrigenous clastic components. Based on low its low $CaCO_3$ content and substantial clastic content, Frey and Bromley (1985) suggested that, in most places, this unit should not be called a “chalk.” The unnamed member of the Mooreville Chalk contains a low-diversity assemblage of ichnofossils, including *Chondrites*, *Thalassinoides*, and *Zoophycos* (Table 6.2). Sedimentologically and ichnologically, this unit differs considerably from the relatively pure Clayton chalk.

The Prairie Bluff Chalk, which is also exposed at Moscow Landing, is a sandy, glauconitic chalk with $CaCO_3$ contents averaging approximately 72% (Morton et al., 2019). This unit contains a Cruziana ichnofacies assemblage dominated by *Chondrites*, *Thalassinoides*, and *Cylindrichnus* (Table 6.2). The sedimentology and ichnology of the Prairie Bluff Chalk are indicative of a relatively shallow, inner shelf setting. The Clayton chalk differs from that of the Prairie Bluff Chalk in that it is finer grained and less clastic rich, contains only very rare glauconite, and is characterized by a more diverse Zoophycos ichnofacies assemblage of traces.

The unnamed lower member of the Demopolis Chalk is the purest chalk in the Selma Group with an average $CaCO_3$ content of approximately 80% (Locklair and Savrda 1998a). It contains variable amounts of clay and only rare mica and very fine quartz (Frey and Bromley, 1985). This unit is characterized by a diverse Zoophycos ichnofacies assemblage (Table 6.2; Locklair and Savrda, 1998a, b; Savrda, 2012, 2014) that is most similar to that documented herein for the Clayton chalk. The Clayton chalk compares most favorably with the Demopolis Chalk with respect to texture, composition, and ichnology. Consequently, like the Demopolis Chalk (Locklair and Savrda, 1998a), the Clayton chalk likely accumulated in a relatively quiet, well-oxygenated outer-shelf setting during a period of relatively high sea-level stand.

6.5.2 Implications for Sea-Level Dynamics

In a sequence stratigraphic context, the Clayton chalk previously has been interpreted to represent the condensed section of sequence TAGC-1.2 (Fig. 6.11;

Mancini and Tew, 1993; Savrda, 1991). This is consistent with its inferred outer-shelf depositional setting and link to a phase of sea-level transgression. The timing of transgression can be estimated based on biostratigraphic context. The Clayton chalk lies in the lower parts of the NP3 nannoplankton zone and the *Subbotina trinidadensis* foraminiferal zone (Mancini and Tew, 1993; Fig. 6.11). In this context, the transgressive event responsible for the Clayton Chalk would have occurred circa 62-63 Myr ago.

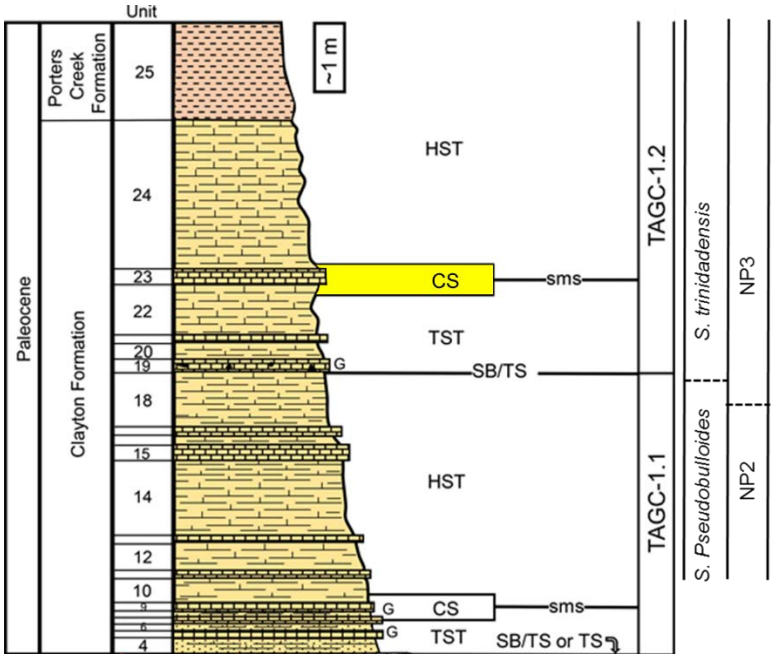

Figure 6.11 – Stratigraphic column depicting sequence stratigraphic and biostratigraphic context of Clayton Formation and Porters Creek Formation exposed at Moscow Landing (modified from Savrda, 2018).

The Clayton chalk may record Briskin and Fluegeman's (1990) TA 1.2A high sea-level stand, which is inferred from benthic foraminiferal assemblages. In their study, Briskin and Fluegeman (1990) examined 101 benthic foraminifera-bearing samples from sedimentary deposits of the Eastern Gulf Coastal Plain of Mississippi, Alabama, and Georgia. While they did not sample of the Clayton chalk described herein, they recognized a significant early Paleocene marine

flooding event during which they assert that sea levels may have been ±240 m above the present level. Briskin and Fluegeman (1990) proposed that this transgressive event occurred approximately 64.2 Myr ago. The potential age discrepancy (between 62-63 Ma vs 64.2 Ma) may be related to the use of different time scales by various authors. Notably, Briskin and Fluegeman (1990) dubbed this early Paleocene transgression as the “Cannonball” event, suggesting a link to transgressive deposits manifest in the U.S. western interior (Cannonball Formation or Cannonball Member of the Fort Union Formation; see below).

6.5.3 Relations to Western Interior/Cannonball Sea

Throughout the Cretaceous, a major interior seaway—the Western Interior seaway—extended from the Gulf coast region northward to the Arctic. The seaway waxed and waned in extent through time and essentially disappeared at the end of the Cretaceous, as evidenced by the transition from marine to continental deposition. However, evidence for an early Paleocene resurgence of the seaway is provided by strata containing marine or marginal marine foraminifera, microbenthic body fossils, and/or trace fossils (Fox and Olsson, 1969; Cvancara, 1976; Belt et al., 1997; Catuneanu et al., 2000; Hartman and Kirkland, 2002; Boyd and Lillegrave, 2011). These strata include the Cannonball Member of the Fort Union Formation (aka Peace Garden Member of Cannonball Formation; Catuneanu et al., 2000), which provided the basis for the recognition of what has been referred to as the Cannonball Sea (Fig. 6.12). The Cannonball Member, exposed in the Williston Basin of the Dakotas and adjacent areas of

Canada, includes three westward-extending tongues of marine shale and fine-grained sandstone that reflect distinct transgressive pulses—in ascending order, the Corbicula, Boyce, and Three V tongues (Belt et al., 2004). The Three V tongue apparently records the most extensive expansion of the Cannonball Sea (Belt et al., 2004).

Figure 6.12 – Early Paleocene (Danian) paleographic map of North America showing the position of the Cannonball Sea in relation to the Gulf of Mexico and Mississippi embayment. Location of Moscow Landing marked with red dot (modified from Slattery et al., 2013).

The exact timing of peak expansion of the Cannonball Sea is poorly defined. For example, paleomagnetic studies alternately assign the Three V tongue to 62.5 Ma (chron C28n; Lund et al., 2002) and 64.1-64.2 Ma (chron C28r; Peppe et al., 2009). Based on pollen, mammalian faunas, and radiometric age dates, Belt et al. (2004) proposed that the Three V transgression occurred circa 64.2 Ma. Despite these discrepancies in inferred timing of peak transgression, most authors agree that the Cannonball Sea persisted to some degree for the first 5 Ma of the Paleocene (65-60 Myr ago; Hartman and Kirkland, 2002; Belt et al., 2004).

The degree to which the Cannonball Sea was connected to the Gulf of Mexico and northern Mississippi embayment is uncertain (Boyd and Lillegrave, 2011; Slattery et al., 2013; Fig. 6.12). However, deposition of the Clayton chalk in Gulf region was at least partly coeval with deposition of the Cannonball Member in the Western Interior, indicating that both are responses to the same early Paleocene transgressive event.

6.5.4 Implications for Paleogeography

This study raises several questions about early Paleocene paleogeography. One of these questions concerns the configuration of the Mississippi embayment during the deposition of the Clayton chalk. On the general Paleocene paleogeographic map generated by Mancini and Tew (1993) for Alabama and Mississippi (Fig. 6.13), the Moscow Landing locality lies very near the approximate updip limit of exposed Paleocene strata. Because the Clayton chalk records outer shelf conditions, it is very likely that during the early

Paleocene the depositional shoreline of Mississippi embayment lay much further north and east of this updip outcrop limit. That is, during the transgressive event recorded by the Clayton chalk, the Mississippian embayment must have been more areally extensive than typically depicted on paleogeographic maps (e.g., Fig. 6.12).

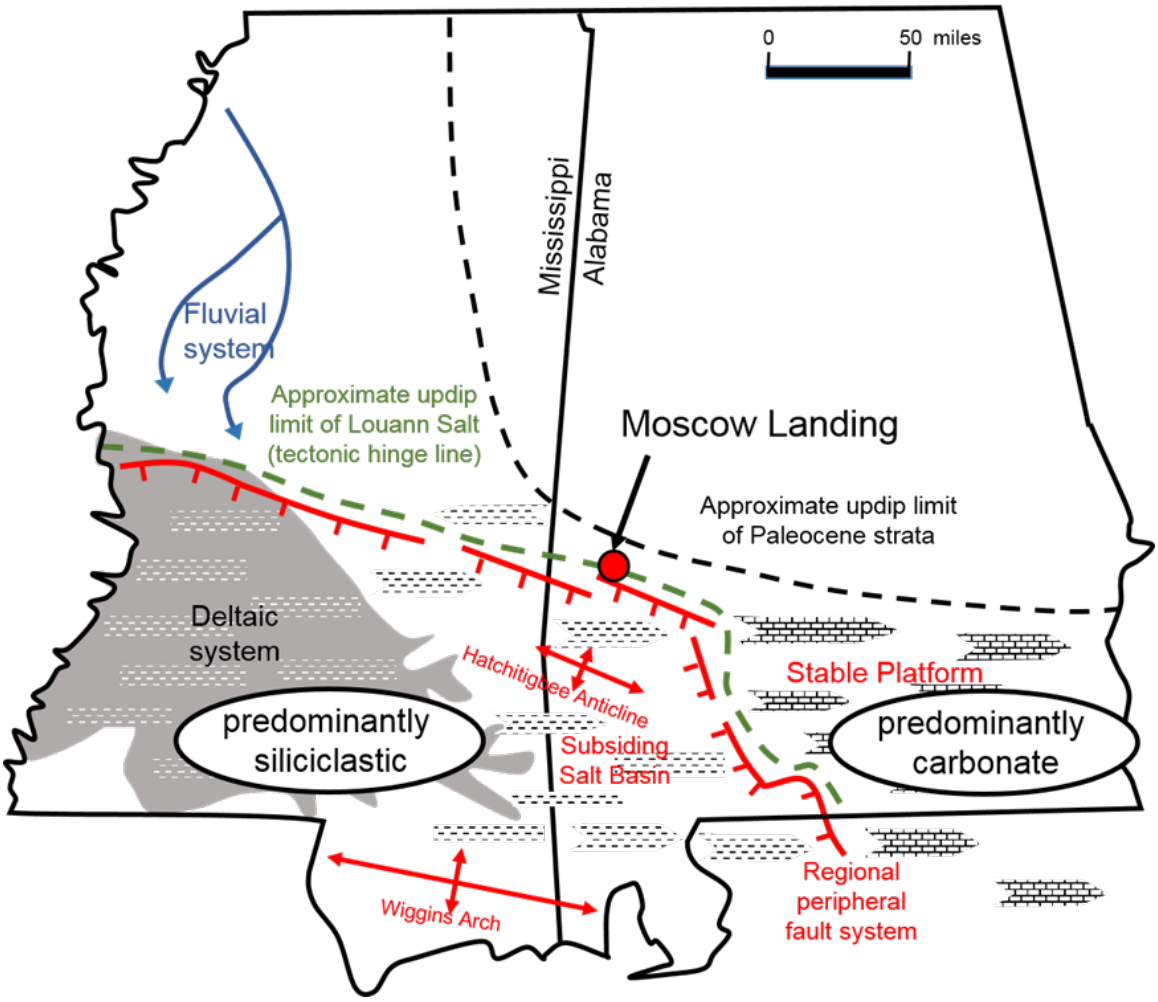

Figure 6.13 – Generalized Paleocene Paleogeography of the Gulf coastal plain (modified from Mancini and Tew, 1993).

A related question concerns the specific events that led to the relatively abrupt shift from slow carbonate ooze deposition (manifest by the Clayton chalk) to clay-dominated clastic deposition represented by the Porters Creek Formation.

Sea-level fall, final draining of interior seaways, and the development of major river-drainage systems resulted in substantial changes in paleogeography and environmental conditions at the Moscow Landing locality. The localized truncation of the Clayton chalk beneath the aforementioned broad scour surface (Fig. 6.4) presumably reflects significant shallowing and, consequently, at least periodic winnowing, perhaps by storm currents, shortly after offshore shelf chalk deposition.

6.6 Summary

The Clayton chalk exposed at the Moscow Landing is a light gray to white, moderately indurated chalk containing a moderately diverse ichnofossil assemblage representing the Zoophycos ichnofacies. When compared to Cretaceous chalk-dominated units of the Selma Group, the Clayton chalk is most similar to the Demopolis Chalk with respect to sediment texture, composition, and ichnofabrics. This suggests that deposition of the Clayton chalk occurred in a relatively quiet, well-oxygenated outer shelf setting and is consistent with the interpretation of the Clayton chalk as a condensed section. Based on biostratigraphic constraints, the transgression responsible for Clayton chalk deposition occurred ~62-63 Myr ago and is in part coeval with the development of the Cannonball Sea in the U.S. Western Interior. The transition from Clayton chalk to clay-dominated Porters Creek deposits reflects relatively abrupt changes in sea-level, paleogeography, and depositional environments along the eastern flank of the Mississippi embayment.

7. Summary

The Moscow Landing section, exposed at low water on the west bank of the Tombigbee River, Sumter County, Alabama, exposes the Upper Cretaceous (Maastrichtian) Prairie Bluff Chalk, the purported K-T boundary impact-induced megawave deposits (Clayton sands), and Lower Paleocene (Danian) Clayton and Porters Creek formations. The overarching goal of this study was to improve our overall understanding of the Moscow Landing section. Below is a synopsis of each of the major objectives: (1) to generate a detailed geologic map of the entire Moscow Landing exposure; (2) to characterize and interpret large burrow systems expressed in an alternating marl-marly limestone sequence in the middle portion of the Clayton Formation; and (3) to characterize the sedimentology and ichnology of a thin chalk bed (Clayton chalk) in the upper part of the Clayton Formation.

7.1 Objective 1

The current research resulted in the first detailed map of the Moscow Landing section. The map depicts the distribution of stratigraphic units and faults in nine partly overlapping segments or strips, each of which encompass ~650 feet of shoreline. Mapped units include, in ascending order, the upper part of the Prairie Bluff Chalk, including a thin, partly phosphatic fossil lag bed therein; several distinct, discontinuous Clayton sand bodies linked to megawave deposition or related sea-level changes; the Clayton Formation, including a chalk

marker bed in its upper part; and the lower part of the Porters Creek Formation. Structural features include 22 faults, most of which strike WNW, dip to the NE or SW at 35-70 degrees, and mainly reflect normal offset. At least three of the faults offset the Prairie Bluff Chalk and the Clayton sand beds but are truncated at the base of the Clayton Formation. While strata generally dip very gently (1-4 degrees) to the south, dips are locally steepened and reversed, particularly adjacent to faults. This map should be of use to future researchers and students who visit this important section.

7.2 Objective 2

The bulk of the Clayton Formation at Moscow Landing is characterized by the alternation of relatively thick (18-120 cm), dark olive-gray, poorly indurated marls and thin, light gray, indurated, locally glauconitic interbeds of marly limestone. Large burrow systems emanating from and passively filled with marly limestones cut across softground ichnofabrics of underlying marls. These areally extensive, predominately horizontal, irregularly branching burrow systems are attributed to extended dwelling and/or feeding activities of one more types of decapod crustaceans. Depending on the presence or absence of burrow-wall scratch traces (bioglyphs), these burrows are most allied with the ichnotaxa *Spongeliomorpha iberica* and *Thalassinoides paradoxicus*, respectively. Both of these forms in the Clayton Formation are indicative of the firmground Glossifungites ichnofacies. Firmground conditions developed in response to erosional exhumation of semiconsolidated marls at parasequence-bounding

marine flooding surfaces, consistent with previous sequence stratigraphic interpretations.

7.3 Objective 3

The Clayton chalk, which occurs a few meters below the contact between the Clayton Formation and Porters Creek Formation, is a light gray to white, moderately indurated, thoroughly bioturbated, foraminiferal wackstone. Ichnofabrics of the chalk and associated piped zone are characterized by a Zoophycos ichnofacies assemblage of traces that include abundant *Chondrites*, common *Thalassinoides*, *Planolites*, *Teichichnus*, and *Zoophycos*, and rare *Phycosiphon*, *Taenidium*, and *Phycosiphon*. Compared to chalk-dominated units of the Cretaceous Selma Group in the eastern Gulf coastal plain, the Clayton chalk is most similar to the Demopolis Chalk with respect to sediment texture, composition, and ichnofabrics. This suggests that the Clayton chalk was deposited in a relatively quiet, well-oxygenated outer-shelf setting and is consistent with the interpretation of the Clayton chalk as a condensed section formed in response to marine transgression. Based on biostratigraphic constraints, the transgression responsible for Clayton chalk deposition occurred ~62-63 Myr ago and is in part coeval with the development of the Cannonball Sea in the U.S. Western Interior. The transition from Clayton chalk to clay-dominated Porters Creek deposits reflects relatively abrupt changes in sea-level, paleogeography, and depositional environments along the eastern flank of the Mississippi embayment.

REFERENCES

Allen, E.A., and Curran, H.A., 1974, Biogenic sedimentary structures produced by crabs in lagoon margin and salt marsh environments near Beaufort, North Carolina: Journal of Sedimentary Research, v. 44, p. 538-548.

Baum, G.R., and Vail, P.R., 1988, Sequence stratigraphic concepts applied to Paleogene outcrops, Gulf and Atlantic basins, *in* Wilgus, C.K., Hastings, B.S., Kendall, C.G.St.C., Posamentier, H.W., Ross, C.A., and Van Wagoner, J.C., eds., Sea-level changes: an integrated approach: Society of Economic Paleontologists and Mineralogists Foundation, Gulf Coast Section, Annual Research Conference, 11th, p. 21-51.

Belaústegui, Z., Gibert, J.M. de, López-Blanco, M., and Bajo, I., 2014, Recurrent constructional pattern of the crustacean burrow *Sinusichnus sinuosus* from the Paleogene and Neogene of Spain: Acta Paleontologica Ponolica, v. 59, p. 461-474.

Belt, E.S., Hartman, J.H., Diemer, J.A., Kroeger, T.J., Tibert, N.E., and Curran, H.A., 2004, Unconformities and age relationships, Tongue River and older members of the Fort Union Formation (Paleocene), western Williston Basin, U.S.A: Rocky Mountain Geology, v. 39, p. 113-140.

Boyd, D.W., and Lillegraven, J.A., 2011, Persistence of the Western Interior Seaway: Historical background and significance of *Rhizocorallium* in Paleocene strata, south-central Wyoming: Rocky Mountain Geology, v. 46, p. 43-69.

Braithwaite, C.J.R. and Talbot, M.R., 1972, Crustacean burrows in the Seychelles, Indian Ocean: Palaeogeography, Palaeoclimatology, Palaeoecology, v. 11, p. 268-285.

Briskin, M., and Fluegeman, R., 1990, Paleocene sea level movements with a 430,000 year quasi-periodic cyclicity: PALAIOS, v. 5, p. 184-198.

Bromley, R.G., 1975, Trace fossils at omission surfaces. In: Frey, R.W. (Ed.), The Study of Trace Fossils. Springer, New York, NY, p. 399-428.

Bromley, R.G., 1991, *Zoophycos*: strip mine, refuse dump, cache or sewage farm?: Lethaia, v. 24, p. 460-462.

Buatois, L.A., and Mángano, M.G., 2011, Ichnology: Organism-substrate interactions in space and time: New York, Cambridge University Press, 358 p.

Carvalho, C.N. de, Viegas, P.A., and Cachão, M., 2007, *Thalassinoides* and its producer: populations of *Mecochirus* buried within their burrow systems, Boca Do Chapim Formation (Lower Cretaceous), Portugal: PALAIOS, v. 22, p. 104-109.

Catuneanu, O., Sweet, A.R., and Miall, A.D., 2000, Reciprocal stratigraphy of the Campanian-Paleocene Western Interior of North America: Sedimentary Geology, v. 134, p. 235-255.

Chapman, C.J. and Rice, A.L., 1971, Some direct observations on the ecology and behavior of the Norway lobster *Nephrops norvegicus*: Marine Biology, v. 10, p. 321-329.

Cvancara, A.M., 1976, Geology of the Cannonball Formation (Paleocene) in the Williston Basin, with reference to Uranium potential: North Dakota Geological Survey, Report of Investigation 57, 22 p.

D'Alessandro, A. and Bromley, R.G., 1995, A new ichnospecies of *Spongeliomorpha* from the Pleistocene of Sicily: Journal of Paleontology, v. 69, p. 393-398.

Ekdale, A.A. and Bromley, R.G., 1984, Comparative ichnology of shelf-sea and deep-sea chalk: Journal of Paleontology, v. 58. P. 322-332.

Ekdale, A.A. and Bromley, R.G., 2003, Paleoethologic interpretation of complex *Thalassinoides* in shallow-marine limestones, Lower Ordovician, southern Sweden: Paleogeography, Palaeoclimatology, Palaeoecology, v. 192, p. 221-227.

Fox, S.K., Jr., and Olsson, R.K., 1969, Danian planktic foraminifera from the Cannonball Formation in North Dakota: Journal of Paleontology, v. 43, p. 1397-1404.

Frey, R.W. and Bromley, R.G., 1985, Ichnology of American chalks: the Selma Group (Upper Cretaceous), western Alabama: Canadian Journal of Earth Science, v. 22, p. 801-828.

Frey, R.W. and Howard, J.D., 1985, Trace fossils from the Panther Member, Star Point Formation (Upper Cretaceous), Coal Creek Canyon, Utah: Journal of Paleontology, v. 59, p. 370-404.

Frey, R.W., Howard, J.D., and Pryor, W.A., 1978, *Ophiomorpha*: Its morphologic, taxonomic, and environmental significance: Paleogeography, Paleoclimatology, Paleoecology, v. 23, p. 199-229.

Gibert, J.M. de, 1996, A new decapod burrow system from the NW Mediterranean Pliocene: Revista Española de Paleontología, v. 11, p. 251-254.

Gibert, J.M. de and Ekdale, A.A., 2010, Paleobiology of the crustacean trace fossil *Spongeliomorpha iberica* in the Miocene of southeastern Spain: Acta Palaeontologica Polonica, v. 55, p. 733-740.

Gibert, J.M. de and Robles, J.M., 2005, Firmground ichnofacies recording high-frequency marine flooding events (Langhian transgression, Vallès-Penedès Basin, Spain): Geologica Acta, v. 3, p. 295-305.

Gingras, M.K., Hubbard, S.M., Pemberton, S.G., and Saunders, T.D.A., 2000, The significance of Pleistocene *Psilonichnus* at Willapa Bay, Washington: Palaios, v. 15, p. 142-151.

Griffis, R.G. and Suchanek, T.H., 1991, A model of burrow architecture and trophic modes in thalassinidean shrimp (Decapoda: Thalassinidea): Marine Ecology Progress Series, v. 79, p. 171-183.

Harrer, J.W. Jr., 1986, The depositional environments and paleoecology of benthic foraminifera in the Clayton Formation (Danian) of Alabama [M.S. Thesis]: Auburn University, 255 p.

Hart, M. B., Harries, P. J., Cárdenas, A.L., 2013, The Cretaceous/Paleogene Boundary Events in the Gulf Coast: Comparisons between Alabama and

Texas: Gulf Coast Association of Geological Societies Transactions, v. 63, p. 235-255.

Hartman, J. H., and Kirkland, J.I., 2002, Brackish and marine mollusks of the Hell Creek Formation of North Dakota: Evidence for a persisting Cretaceous seaway, *in* Hartman, J.H., Johnson, K.R., and Nichols, D.J., eds., The Hell Creek Formation and the Cretaceous-Tertiary boundary in the northern Great Plains region: An integrated continental record of the end of the Cretaceous: Geological Society of America Special Paper 361, p. 271-296.

Hayasaka, I., 1935, The burrowing activities of certain crabs and their geologic significance: The American Midland Naturalist, v. 16, p. 99-103.

Hill, G.W. and Hunter, R.E., 1973, Burrows of the ghost crab Ocypode quadrata (Fabricius) on the barrier islands, south-central Texas coast: Journal of Sedimentary Research, v. 43, p. 24-30.

Howard, J.D. and Frey, R.W., 1984, Characteristic trace fossils in nearshore to offshore sequences, Upper Cretaceous of east-central Utah: Canadian Journal of Earth Sciences, 1984, v. 21, p. 200-219.

Kinoshita, K., 2002, Burrow structure of the mud shrimp *Upogebia major* (decapoda: thalassinidea: upogebiidae): Journal of Crustacean Biology, v. 22, p. 474-480.

Knaust, D., Uchman, A, and Hagdorn, H, 2016, The probable isopod burrow *Sinusichnus seilacheri* isp. n. from the Middle Triassic of Germany: an example of behavioral convergence: Ichnos, v. 23, p. 134-146.

Locklair, R.E. and Savrda, C.E., 1998a, Ichnology of rhythmically bedded Demopolis Chalk (Upper Cretaceous, Alabama): implications for Paleoenvironment, depositional cycle origins, and tracemaker behavior: PALAIOS, v. 13, p. 423-438.

Locklair, R.E. and Savrda, C.E., 1998b, Ichnofossil tiering analysis of a rhythmically bedded chalk-marl sequence in the Upper Cretaceous of Alabama: Lethaia, v. 31, p. 311-322.

Lund, S.P., Hartman, J.H., and Banerjee, S.K., 2002, Magnetostratigraphy of interfingering Upper Cretaceous-Paleocene marine and continental strata of the Williston Basin, North Dakota and Montana, *in* Hartman, J.H., Johnson, K.R., and Nichols, D.J., eds., The Hell Creek Formation and the Cretaceous-Tertiary boundary in the northern Great Plains region: An integrated continental record of the end of the Cretaceous: Geological Society of America Special Paper 361, p. 57-74.

MacEachern, J.A., Raychaudhuri, I., and Pemberton, S.G., 1992, Stratigraphic applications of the *Glossifungites* ichnofacies: Delineating discontinuities in the rock record: *in* Pemberton, S.G., ed., Applications of Ichnology to Petroleum Exploration, a Core Workshop: Society of Economic Paleontologists and Mineralogists Core Workshop 17, 169-198.

Mancini, E.A., and Tew, B.H., 1988, Paleocene sequence Stratigraphy of southwestern Alabama: Gulf Coast Association of Geological Societies Transactions, v. 38, p. 453-460.

Mancini, E.A., and Tew, B.H., 1993, Eustasy versus subsidence: Lower Paleocene depositional sequences from southern Alabama, eastern Gulf Coastal Plain: Geological Society of America Bulletin, v. 105, p. 3-17.

Melchor, R.N., Bromley, R.G., and Bedatou, E., 2010, *Spongeliomorpha* in nonmarine settings: an ichnotaxonomic approach: Earth and Environmental Science Transactions of the Royal Society of Edinburgh, v. 11, p. 429-436.

Miller, M.F. and Curran, H.A., 2001, Behavioral plasticity of modern and Cenozoic burrowing thalassinidean shrimp: Palaeogeography, Palaeoclimatology, Palaeoecology, v. 166, p. 219-236.

Morton, C., Savrda, C.E., and Foster, C.B., 2019, Preliminary observations of carbonate depositional rhythms in part of the Upper Cretaceous Prairie Bluff Chalk, Moscow Landing, Sumter County, Western Alabama: Geological Society of America Abstracts with Programs, v. 51, no. 3.

Nickell, L.A. and Atkinson, R.J.A., 1995, Functional morphology of burrows and trophic modes of three thalassinidean shrimp species, and a new approach to the classification of thalassinidean burrow morphology: Marine Ecology Progress Series, v. 128, p. 181-197.

Pemberton, S.G. and Frey, R.W., 1985, The *Glossifungites* ichnofacies: Modern examples from the Georgia coast, U.S.A.: *in* Curran, H.A., ed., Biogenic Sedimentary Structures: Their Use in Interpreting Depositional Environments: Society of Economic Paleontologists and Mineralogists, Special Publication no. 35, p. 237-259.

Peppe, D.J., Evans, D.A.D., and Smirnov, A.V., 2009, Magnetostratigraphy of the Ludlow Member of the Fort Union Formation (Lower Paleocene) in the Williston Basin, North Dakota: Geological Society of America Bulletin, January/February 2009, p. 65-79.

Pervesler, P, and Hohenegger, J., 2006, Orientation of crustacean burrows in the Bay of Panzano (Gulf of Trieste, Northern Adriatic Sea): LETHAIA, v. 39, p. 173-186.

Savrda, C.E., 1991, Ichnology in sequence stratigraphic studies: an example from the Lower Paleocene of Alabama: PALAIOS, v. 6, p. 39-53.

Savrda, C.E., 2012, Chalk and related deep-marine carbonates, *in* Knaust, D., and Bromley, R.G., eds., Developments in Sedimentology: Amsterdam, Elsevier, p. 777-806.

Savrda, C.E., 2014, Limited ichnologic fidelity and temporal resolution in pelagic sediments: paleoenvironmental and paleoecologic implications: PALAIOS, v. 29, p. 210-217.

Savrda, C.E., 2018, Revisiting the origins of Clayton sand bodies at the K-Pg transition, Moscow Landing, western Alabama: Stratigraphic relations, sedimentology, and ichnology: PALAIOS, v. 33, p. 555-567.

Schlirf, M., 2000, Upper Jurassic trace fossils from the Boulonnais (northern France): Geologica et Palaeontologica, v. 34, p. 145-213.

Slattery, J.S., Cobban, W.A., McKinney, K.C., Harries, P.J., and Sandness, A.L., 2013, Early Cretaceous to Paleocene paleogeography of the Western Interior Seaway: the interaction of eustasy and tectonism, *in* Woods, A., and Lawlor, J., eds., Wyoming Geological Association Guidebook, p. 22-60.

Smit, J., Roep, Th. B., Alvarez, W., Montanari, A., Claeys, P., Grajeles-Nishimura, J.M., and Bermudez, J., 1996, Coarse-grained, clastic sandstone complex at the K/T boundary around the Gulf of Mexico: Deposition by tsunami waves induced by the Chicxulub impact?: *in* Ryder, G., Fastovsky, D., and Gartner, S., eds., The Cretaceous-Tertiary Event and Other Catastrophes in Earth History: Boulder, Colorado, Geological Society of America Special Paper 307, p. 151-182.

Smith, C.C., 1997, The Cretaceous-Tertiary boundary at Moscow Landing, West-Central Alabama: Geological Survey of Alabama, v. 47, p. 533-540.

Szabo, M.W., and Beg, M.A., 1977, Chalk resources of west-central Alabama: Tuscaloosa, Alabama, Geological Survey of Alabama, 15 p.

Tamaki, A., and Ueno, H., 1998: Burrow morphology of two callianassid shrimps, *Callianassa japonica* Ortman, 1891 and *Callianassa* sp. (=*C. japonica*: de Man, 1928) (Decapoda: Thalassinidea): Crustacean Research, v. 27, p. 28-39.